Bounds on the natural frequencies of laminated rectangular plates with extension-twisting (and shearing-bending) coupling.

Daokui Li[1] and Christopher B. York[2]

Aerospace Sciences, School of Engineering, University of Glasgow, University Avenue, G12 8QQ, Glasgow, Scotland.

Abstract

Anti-symmetric angle-ply laminates are widely believed to uniquely possess *Extension-Twisting* (together with *Shearing-Bending*) coupling behaviour. The results in this article serve to dispel this misconception by presenting solutions for both standard laminates, containing combinations of angle plies (±45°) and cross plies (90° and/or 0°), and angle-ply laminates, containing only ±45° ply orientations; chosen to reflect current industrial design practice, and also because they serve to produce hygro-thermally curvature-stable properties in some standard laminate configurations, i.e., with immunity to the thermal distortions that generally arise in this class of mechanically coupled laminate as a result of the high temperature curing process.

Details of the algorithm used to develop the definitive list of laminate stacking sequences, with up to 21 plies, are given first. Closed form natural frequency solutions for each of these sub-groups are then presented, identifying significant differences in the frequency spectrum bounds across a range of aspect ratios, with respect to the ubiquitous anti-symmetric angle-ply designs.

Keywords

Mechanically coupled laminates, Anti-symmetric, Non-symmetric, Natural Frequency, Warp-free.

1. Introduction

The use of laminated composite materials continues to expand at pace beyond traditional aerospace applications, where the focus remains primarily on strength-to-weight ratio advantage

[1] Permanent address: College of Aerospace Science and Engineering, National University of Defence Technology, Changsha, 410073, China. E-mail address: lidaokui@nudt.edu.cn
[2] Corresponding author: Tel: +44 (0)141 3304345, E-mail address: Christopher.York@Glasgow.ac.uk

over metallic material counterparts. This expansion is due, in part, to a growing awareness of the unique and largely unexploited thermo-mechanical properties that are a potential enabling technology. However, manufacturing constraints continue to restrict design practice to simple design rules, such as the use of symmetric laminates, in order to avoid the undesirable warping distortions that may otherwise result from the high temperature curing process.

Recent research has demonstrated that laminate symmetry is an unnecessary constraint in developing fully uncoupled properties [1,2], commonly referred to as *black-metal*, and that non-symmetric laminates, with mechanically coupled behaviour, can also be achieved with immunity to thermal warping distortions [3]. The continuing perception that non-symmetric laminates lead to thermal warping distortions has almost certainly led to waning interest in exotic mechanical coupling behaviour in the past, but this topic is now beginning to attract interest as the possibility of tapered, mechanically coupled laminates with immunity to thermal warping distortions have now been realised [4,5], thus offering scope for practical design solutions. Indeed, there are a number of immerging applications that require very specific mechanically coupled properties. Tilt-rotor blades provide an example of one such application, where mechanical extension-twisting coupling at the structural (or blade) level is used to develop an optimized twist distribution along the blade for both hover and forward flight: a change in rotor speed, and the resulting centrifugal force, provides the required twist differential between the two flight regimes. In early designs, this behaviour was achieved from laminate level extension-shearing coupling, developed simply from off-axis alignment of a balanced and symmetric laminate [6]. However, whilst laminate symmetry ensures immunity to thermal warping, these designs result in significant bending-twisting coupling at the laminate level, leading to detrimental effects on the compression buckling strength of the blade, which may be an active design constraint when the blade is parked. An alternative is to adopt a laminate design with extension-twisting coupling, but in general, this class of laminate requires specially curved tooling in order to develop the correct shape after high temperature curing and shape

changes may also arise due to in-service temperature fluctuations. However, a unique sub-class of laminate with extension-twisting coupling has recently been shown [7-8] to be immune to such thermal warping distortions. The discovery of this so called Hygro-Thermally Curvature-Stable or HTCS coupled laminate class has had a strong influence on subsequent studies in the literature, including: maximizing the extension-twisting coupling response [9,10] and/or; integrating additional forms of mechanical coupling response, e.g. bending-twisting coupling [11].

Buckling strength and natural frequency are important indices in the design of structures such as the tilt-rotor blades described above, and closed form solutions, which aid preliminary design for compression buckling strength and natural frequency assessment of simply supported rectangular plates or long prismatic blade structures are well known and well documented in the literature for both isotropic and uncoupled laminated composite materials [12-14]. Less well known are closed form solutions for coupled laminates, derived previously for cross-ply laminates [15] possessing extension-bending coupling, and for angle-ply laminates, with extension-twisting and shearing-bending coupling [16,17]. This is perhaps due to widespread misunderstanding of coupled laminate behaviour, highlighted by Leissa [18], where many buckling results have been presented on the false assumption that bifurcation buckling can occur, when in fact simply supported rectangular plates consisting of cross-ply laminates with extension-bending coupling will bend, and not buckle, when subject to in-plane compressive load. This message appears to have gone unheeded by some [19]. Only the natural frequency predictions remain valid for this class of coupled laminate; a laminate class which is therefore arguably functional rather than structural in nature. Misunderstanding of coupled laminates also extends to the widely held assumptions that extension-twisting (and shearing-bending) coupling is restricted to anti-symmetric angle-ply laminates. Here, the association between mechanical coupling behaviour and laminate symmetry is misleading, particularly in view of the fact that many fully uncoupled anti-symmetric angle-ply laminates have now been identified [1], e.g. the

fully uncoupled anti-symmetric angle-ply laminate: $[45/-45_2/45]_A$. Furthermore, angle-ply laminates will be shown to represent only a small subset of this class of coupled laminate; the majority of the configurations represent standard laminates, defined as containing combinations of both cross-plies and angle-plies. This is an important discovery, particularly if the larger design space leads to a significant change in the bounds on the natural frequencies, or significantly influences the pass bands in wave propagation problems [20].

In this article therefore, definitive listings of laminate configurations with extension-twisting coupling are derived for up to 21 plies, deemed to represent thin laminates. All plies are assumed to possess identical fibre-matrix properties, e.g. carbon-epoxy or glass-epoxy, etc., with constant thickness throughout, differing only by their orientations. The listings comprise individual stacking sequences, separated into angle-ply laminates, representing the generally assumed (anti-symmetric) form for this class of laminate, and standard laminates, deemed to represent laminates containing cross-ply and angle-ply combinations with standard orientations, i.e., 90 and/or 0, +45, -45°. In both cases, no constraint is imposed on the form of sub-sequence symmetry.

The stacking sequences are given in symbolic form since the angle-plies (+/–) can in fact be assigned any arbitrary orientation, $0 < \theta < 90°$, and the cross-plies (●/○) can be interchanged. This is not the case however, for HTCS laminates, which contain standard orientation, defined above, and to which an off-axis material alignment must be applied to achieve the correct coupling characteristics. Each stacking sequence is presented together with a set of non-dimensional parameters, derived in Section 2, from which the laminate stiffness properties can be readily determined for any fibre-matrix system.

Section 3 presents the relevant background theory and the derivation of the closed form solution used to calculate the natural frequency results that then follow. Section 4 presents the frequency bounds for HTCS or warp-free laminates, which are compared with those for both standard and angle-ply laminates. These comparisons involve the upper- and lower-bounds on the first three

natural frequencies for Extension-Twisting (and Shearing-Bending) coupled laminates, over a broad range of aspect ratios. Warp-free laminates can be manufactured using a high temperature curing system without introducing unwanted thermal distortions on cooling; they are also free from such distortions in service. The standard and angle-ply laminates presented require either special curved tooling or cold cure resin systems to achieve the desired shape after manufacture and are subject to thermal distortions in service.

2. Extension-Twisting (and Shearing-Bending) coupled laminates.

2.1 *Laminate characterization.*

Laminated composite materials have recently been characterized [2] in terms of their response to mechanical and/or thermal loading, to help understand coupling behaviour not present in conventional materials. Equation (1) describes the well-known **ABD** relation from classical lamination theory, relating force {**N**} and moment {**M**} resultants with in-plane strains {**ε**} and curvatures {**κ**}, and from which the coupling behaviour is, by inspection, dependent on the form of the elements, A_{ij}, B_{ij} and D_{ij}, of the extensional [**A**], coupling [**B**] and bending [**D**] stiffness matrices, respectively:

$$\begin{Bmatrix} N_x \\ N_y \\ N_{xy} \end{Bmatrix} = \begin{bmatrix} A_{11} & A_{12} & A_{16} \\ & A_{22} & A_{26} \\ \text{Sym.} & & A_{66} \end{bmatrix} \begin{Bmatrix} \varepsilon_x \\ \varepsilon_y \\ \gamma_{xy} \end{Bmatrix} + \begin{bmatrix} B_{11} & B_{12} & B_{16} \\ & B_{22} & B_{26} \\ \text{Sym.} & & B_{66} \end{bmatrix} \begin{Bmatrix} \kappa_x \\ \kappa_y \\ \kappa_{xy} \end{Bmatrix}$$
$$\begin{Bmatrix} M_x \\ M_y \\ M_{xy} \end{Bmatrix} = \begin{bmatrix} B_{11} & B_{12} & B_{16} \\ & B_{22} & B_{26} \\ \text{Sym.} & & B_{66} \end{bmatrix} \begin{Bmatrix} \varepsilon_x \\ \varepsilon_y \\ \gamma_{xy} \end{Bmatrix} + \begin{bmatrix} D_{11} & D_{12} & D_{16} \\ & D_{22} & D_{26} \\ \text{Sym.} & & D_{66} \end{bmatrix} \begin{Bmatrix} \kappa_x \\ \kappa_y \\ \kappa_{xy} \end{Bmatrix} \quad (1)$$

where the force and moment resultant vector components account for the combined effects of thermal, mechanical and hygral loading.

The coupling behaviour can be described by a shorthand notation, using an extended subscript notation defined previously by the Engineering Sciences Data Unit [21]. Balanced and anti-

symmetric angle-ply laminates are referred to by the designation $\mathbf{A}_S\mathbf{B}_t\mathbf{D}_S$, signifying that the extensional stiffness matrix [**A**] is *Simple* in nature, i.e., uncoupled, since

$$A_{16} = A_{26} = 0, \tag{2}$$

the coupling matrix [$\mathbf{B}_t$] has non-zero off-diagonal, or *transverse* elements, i.e.,

$$B_{16}, B_{26} \neq 0, \tag{3}$$

with all other elements zero, and the bending stiffness matrix [$\mathbf{D}_S$] is *Simple* in nature, i.e., uncoupled, since

$$D_{16} = D_{26} = 0. \tag{4}$$

Alternatively, coupled laminates may also be described in terms of the response that they exhibit under various combinations of force and moment resultants (or equally, the force and moment resultants that arise from enforced strains or curvatures), using a *cause-effect* relationship. Balanced and anti-symmetric angle-ply laminates may therefore be described as *E-T-S-B* laminates, since *Extension* (*E*) causes a *Twisting* (*T*) effect and *Shearing* (*S*) causes a *Bending* (*B*) effect. Each *cause-effect* pair is reversible, e.g. *T-E-B-S*, and are underlined for clarity, since the two coupling relationships are inseparable for this class of coupled laminate. Note that this response-based labelling is complementary to the Engineering Sciences Data Unit subscript notation [21].

2.2 *Derivation of Extension-Twisting (and Shearing-Bending) coupled laminates.*

In what follows, the general rules of symmetry are relaxed, hence cross plies (0° and 90°) and angle plies (45° and -45°) are not constrained to be anti-symmetric about the laminate mid-plane. Symbolic notation is adopted to allow for non-standard ply orientations, although with the exception of a small number of validation studies presented at the beginning of Section 4, all results presented do in fact relate to standard ply angle orientations, ±45°, 90° and/or 0°. All stacking sequences have an angle-ply (+) on one surface (1st ply) of the laminate, but the other

surface ply may have equal (+) or opposite (–) orientation or it may indeed be a cross ply (○ or ●) of 0 or 90° orientation.

Non-dimensional parameters are adopted to allow for any fiber/matrix system. The derivation of non-dimensional coupling stiffness parameters is readily demonstrated for the example of a 9-ply laminate, with non-symmetric stacking sequence $[+/○/–/○/+_2/–_2/○]_T$, where elements of coupling stiffness matrix,

$$B_{ij} = \Sigma Q'_{ij,k}\,(z_k^{\,2} - z_{k-1}^{\,2})/2 \qquad (5)$$

where the summation may instead be written in sequence order for the (k = 1, 2, ..,) 9 individual plies, and where z, representing the distance from the laminate mid-plane, is expressed here in terms of the uniform ply thickness, t, see Fig.1:

$$\begin{aligned} B_{ij} = \{&Q'_{ij+}((-7t/2)^2 - (-9t/2)^2) + Q'_{ij○}((-5t/2)^2 - (-7t/2)^2) + Q'_{ij–}((-3t/2)^2 - (-5t/2)^2) \\ &+ Q'_{ij○}((-t/2)^2 - (-3t/2)^2) + Q'_{ij+}((t/2)^2 - (-t/2)^2) + Q'_{ij+}((3t/2)^2 - (t/2)^2) \\ &+ Q'_{ij–}((5t/2)^2 - (3t/2)^2) + Q'_{ij–}((7t/2)^2 - (5t/2)^2) + Q'_{ij○}((9t/2)^2 - (7t/2)^2)\}/2 \end{aligned} \qquad (6)$$

and Q'_{ij+}, $Q'_{ij–}$, and $Q'_{ij○}$, with subscripts i,j = 1, 2, 6, corresponds to the transformed reduced stiffnesses for ply angle orientations +45°, -45° and 0°, respectively.

The coupling stiffness contributions for each ply orientations may be summarised as:

$$\begin{aligned} B_{ij+} &= -6t^2/2 \times Q'_{ij+} = \chi_+ t^2/4 \times Q'_{ij+} \\ B_{ij–} &= 6t^2/2 \times Q'_{ij–} = \chi_– t^2/4 \times Q'_{ij–} \\ B_{ij○} &= 0t^2/2 \times Q'_{ij○} = \chi_○ t^2/4 \times Q'_{ij○} \end{aligned} \qquad (7)$$

where $\chi_+ = -\chi_– = -12$, $\chi_○ = 0$ (and $\chi_● = 0$).

Similar non-dimensional parameters can be developed for the extensional and bending stiffness matrices. These non-dimensional parameters, together with the transformed reduced stiffness, Q'_{ij}, for each ply orientation with constant ply thickness, t, facilitate simple calculation of the elements of the extensional, coupling and bending stiffness matrices from:

$$A_{ij} = \{n_{+}Q'_{ij+} + n_{-}Q'_{ij-} + n_{○}Q'_{ij○} + n_{●}Q'_{ij●}\}t$$

$$B_{ij} = \{\chi_{+}Q'_{ij+} + \chi_{-}Q'_{ij-} + \chi_{○}Q'_{ij○} + \chi_{●}Q'_{ij●}\}t^2/4 \quad (8)$$

$$D_{ij} = \{\zeta_{+}Q'_{ij+} + \zeta_{-}Q'_{ij-} + \zeta_{○}Q'_{ij○} + \zeta_{●}Q'_{ij●}\}t^3/12$$

For Extension-Twisting (and Shearing-Bending) coupling, i.e., B_{16}, $B_{26} \neq 0$ (with all other B_{ij} = 0):

$$\chi_{+} = -\chi_{-} \text{ and } \chi_{○} = \chi_{●} = 0 \quad (9)$$

It is important to note that Eq (9) does not imply that cross plies (○ or ●) are absent, as has been the assumption in all previous studies on this class of coupled laminate.

For uncoupled Extensional stiffness properties, i.e., $A_{16} = A_{26} = 0$ the number of angle plies satisfy the condition:

$$n_{+} = n_{-} \quad (10)$$

and for uncoupled Bending stiffness properties, $D_{16} = D_{26} = 0$ the non-dimensional bending stiffness parameters, representing angle plies, satisfy the condition:

$$\zeta_{+} = \zeta_{-} \quad (11)$$

A proof for these constraints is provided in the electronic annex to this article.

The transformed reduced stiffness relationships are defined by:

$$\begin{aligned}
Q'_{11} &= Q_{11}\cos^4\theta + 2(Q_{12} + 2Q_{66})\cos^2\theta\sin^2\theta + Q_{22}\sin^4\theta \\
Q'_{12} &= Q'_{21} = (Q_{11} + Q_{22} - 4Q_{66})\cos^2\theta\sin^2\theta + Q_{12}(\cos^4\theta + \sin^4\theta) \\
Q'_{16} &= Q'_{61} = \{(Q_{11} - Q_{12} - 2Q_{66})\cos^2\theta + (Q_{12} - Q_{22} + 2Q_{66})\sin^2\theta\}\cos\theta\sin\theta \\
Q'_{22} &= Q_{11}\sin^4\theta + 2(Q_{12} + 2Q_{66})\cos^2\theta\sin^2\theta + Q_{22}\cos^4\theta \\
Q'_{26} &= Q'_{62} = \{(Q_{11} - Q_{12} - 2Q_{66})\sin^2\theta + (Q_{12} - Q_{22} + 2Q_{66})\cos^2\theta\}\cos\theta\sin\theta \\
Q'_{66} &= (Q_{11} + Q_{22} - 2Q_{12} - 2Q_{66})\cos^2\theta\sin^2\theta + Q_{66}(\cos^4\theta + \sin^4\theta)
\end{aligned} \quad (12)$$

where θ is the ply angle orientation, and the reduced stiffness terms are calculated:

$$Q_{11} = E_1/(1 - \nu_{12}\nu_{21})$$

$$Q_{12} = \nu_{12}E_2/(1 - \nu_{12}\nu_{21})$$

$$Q_{22} = E_2/(1 - \nu_{12}\nu_{21}) \quad (13)$$

$$Q_{66} = G_{12}$$

where E_1, E_2, G_{12}, ν_{12}, and ν_{21} are the engineering constants. The reduced stiffness terms, Q_{ij}, can also be related to laminate invariants, U_i:

$$U_1 = \{3Q_{11} + 3Q_{22} + 2Q_{12} + 4Q_{66}\}/8$$

$$U_2 = \{Q_{11} - Q_{22}\}/2$$

$$U_3 = \{Q_{11} + Q_{22} - 2Q_{12} - 4Q_{66}\}/8 \quad (14)$$

$$U_4 = \{Q_{11} + Q_{22} + 6Q_{12} - 4Q_{66}\}/8$$

$$U_5 = \{Q_{11} + Q_{22} - 2Q_{12} + 4Q_{66}\}/8$$

and to the relevant extensional $[A_{ij}]$, coupling $[B_{ij}]$ and bending $[D_{ij}]$ stiffness elements of the **ABD** matrix are given by:

$$A_{11}=\{U_1+\xi_1 U_2+\xi_2 U_3\}H$$

$$A_{12}=A_{21}=\{-\xi_2 U_3+U_4\}H$$

$$A_{22}=\{U_1-\xi_1 U_2+\xi_2 U_3\}H \quad (15)$$

$$A_{66}=\{-\xi_2 U_3+U_5\}H$$

$$B_{16}=B_{61}=\{\xi_7 U_2/2+\xi_8 U_3\}H^2/4$$

$$B_{26}=B_{62}=\{\xi_7 U_2/2-\xi_8 U_3\}H^2/4 \quad (16)$$

$$D_{11}=\{U_1+\xi_9 U_2+\xi_{10} U_3\}H^3/12$$

$$D_{12}=D_{21}=\{U_4-\xi_{10} U_3\}H^3/12 \quad (17)$$

$$D_{22}=\{U_1-\xi_9 U_2+\xi_{10} U_3\}H^3/12$$

$D_{66}=\{-\xi_{10}U_3+U_5\}H^3/12$

where H is the overall thickness of the laminate.

These stiffness elements involve only 6 of the 12 lamination parameters, ξ_i, originally conceived by Tsai and Hahn [22], due to the reduced complexity of the *E-T-S-B* coupled laminate class considered here and only 5 lamination parameters are required (since $\xi_8 = 0$) when stacking sequences contain standard ply orientations, i.e., ±45, 90 and/or 0°.

Lamination parameters introduce ply angle dependency to the previously derived non-dimensional parameters as demonstrated by the following expressions:

$$\begin{aligned}\xi_1 &= \{n_+\cos(2\theta_+) + n_-\cos(2\theta_-) + n_\circ\cos(2\theta_\circ) + n_\bullet\cos(2\theta_\bullet)\}/n\\ \xi_2 &= \{n_+\cos(4\theta_+) + n_-\cos(4\theta_-) + n_\circ\cos(4\theta_\circ) + n_\bullet\cos(4\theta_\bullet)\}/n\end{aligned} \tag{18}$$

$$\begin{aligned}\xi_7 &= \{\chi_+\sin(2\theta_+) + \chi_-\sin(2\theta_-) + \chi_\circ\sin(2\theta_\circ) + \chi_\bullet\sin(2\theta_\bullet)\}/n^2\\ \xi_8 &= \{\chi_+\sin(4\theta_+) + \chi_-\sin(4\theta_-) + \chi_\circ\sin(4\theta_\circ) + \chi_\bullet\sin(4\theta_\bullet)\}/n^2\end{aligned} \tag{19}$$

$$\begin{aligned}\xi_9 &= \{\zeta_+\cos(2\theta_+) + \zeta_-\cos(2\theta_-) + \zeta_\circ\cos(2\theta_\circ) + \zeta_\bullet\cos(2\theta_\bullet)\}/n^3\\ \xi_{10} &= \{\zeta_+\cos(4\theta_+) + \zeta_-\cos(4\theta_-) + \zeta_\circ\cos(4\theta_\circ) + \zeta_\bullet\cos(4\theta_\bullet)\}/n^3\end{aligned} \tag{20}$$

The *Extension-Twisting* (and *Shearing-Bending*) laminate class presented here can be developed by filtering a given set of stacking sequences through the following non-dimensional parameter or associated lamination parameter constraints (derived in the electronic annex to this article):

$$\begin{aligned} &n_+ = n_- && \xi_3 = \xi_4 = 0\\ &\chi_\bullet = \chi_\circ = 0 && \xi_5 = \xi_6 = 0\\ &\chi_+ = -\chi_- && \xi_7U_2/2 + \xi_8U_3 \neq 0\\ & && \xi_7U_2/2 - \xi_8U_3 \neq 0\end{aligned} \tag{21}$$

$\zeta_+ = \zeta_-$ $\xi_{11} = \xi_{12} = 0$

In the derivation of the stacking sequences for laminates with *Extension-Twisting* (and *Shearing-Bending*) coupling, it has been assumed that all plies have identical material properties and ply thickness, *t*, and differ only with respect to ply orientation. The heuristic design constraint of one outer surface angle-ply is also applied, to avoid outer surface cross-ply blocking. Outer surface cross-ply layers may have no effect on the fundamental behavior of the laminate if symmetrically stacked, but are not representative of standard design practice.

Table 1 provides details of the numbers of unique solutions for Extension-Twisting coupled laminates, arising from the parameter constraints of Eq. (21). These solutions represent standard laminates containing ply angle combinations ±45, 90 and/or 0° across the range of ply number (n) groupings investigated, i.e. $2 \leq n \leq 21$. The number of solutions containing angle plies only, and generally described in the literature as anti-symmetric angle-ply laminates, are also presented, together with the number, in parentheses, that are non-symmetric. It should be noted that a description of the stacking sequence symmetry offers no reliable indication of the likely laminate behavior, e.g., the 8-ply anti-symmetric laminate $[+/-_2/+]_A$ possesses fully uncoupled properties.

The vast majority of $\mathbf{A}_S\mathbf{B}_t\mathbf{D}_S$ laminates, with Extension-Twisting coupling, are represented by standard laminates rather than angle-ply (only) laminates. As an example, abridged stacking listings, including non-dimensional parameters are given for 12-layer standard and angle-ply $\mathbf{A}_S\mathbf{B}_t\mathbf{D}_S$ laminates in Tables 2 and 3, respectively. The stacking sequences are ranked in order of increasing Extension-Twisting coupling magnitude. One of the four non-symmetric angle ply laminates identified in Table 1, for this ply number grouping, is presented as stacking sequence 30 in Table 3.

2.3 ***Hygro-Thermally Curvature Stable laminates.***

Hygro-thermally curvature-stable laminates have been shown elsewhere [3] to require square symmetry in both extensional [**A**] and coupling [**B**] stiffness, or the equivalent lamination parameter relationship:

$$\begin{bmatrix} A_{11} & A_{12} & 0 \\ A_{21} & A_{11} & 0 \\ 0 & 0 & (A_{11}-A_{12})/2 \end{bmatrix} \qquad \xi_1 = \xi_2 = \xi_3 = 0$$

$$\begin{bmatrix} 0 & 0 & B_{16} \\ 0 & 0 & -B_{16} \\ B_{16} & -B_{16} & 0 \end{bmatrix} \qquad \xi_5 = \xi_6 = \xi_7 = 0 \qquad (22)$$

These $\mathbf{A_S B_t D_S}$ laminate stiffness relationships cannot be achieved from the laminate class derived above. They arise instead by applying off-axis alignment, $\beta = \pi/8$ or $\beta = -\pi/8$, to a different laminate class, i.e. $\mathbf{A_I B_S D_F}$ laminates with *B-E*-*T-S*;*B-T* coupling or $\mathbf{A_I B_S D_I}$ laminates with *B-E*-*T-S* coupling, with otherwise standard-ply configurations, i.e. $\beta \pm 45°$, $\beta + 0°$ and $\beta + 90°$. Details on these hygro-thermally curvature-stable configurations are given elsewhere [3], however, the number of applicable solutions are summarised in Table 4. These solutions represent the only laminates that can be manufactured flat using a high temperature curing system. It is therefore of interest to compare the bounds of the natural frequencies with standard and angle-ply $\mathbf{A_S B_t D_S}$ laminates, which require special curved tooling to achieve the correct cured shape, yet are still subject to in-service warping distortions due to temperature fluctuations.

3. Background theory on plate vibration for coupled laminates.

Under the Kirchhoff-Love thin plate assumptions, the equilibrium equations for the vibration of a laminated plate with Extension-Twisting and Shearing-Bending (*E-T*-*S-B*) coupling, are:

$$\partial N_x/\partial x + \partial N_{xy}/\partial y = 0$$

$$\partial N_{xy}/\partial x + \partial N_y/\partial y = 0$$

$$\partial^2 M_x/\partial x^2 + 2\partial^2 M_{xy}/\partial x\partial y + \partial^2 M_y/\partial y^2 = \rho\partial^2 w/\partial t^2 \qquad (23)$$

Here, ρ is the mass per mid-plane area. The force $\{\mathbf{N}\} = \{N_x, N_x, N_{xy}\}$ and moment $\{\mathbf{M}\} = \{M_x, M_x, M_{xy}\}$ resultants are related to the mid-plane strains $\{\boldsymbol{\varepsilon}\} = \{\varepsilon_x, \varepsilon_x, \gamma_{xy}\} = \{\partial u/\partial x, \partial v/\partial y, \partial u/\partial y + \partial v/\partial x\}$ and curvatures $\{\boldsymbol{\kappa}\} = \{\kappa_x, \kappa_x, \kappa_{xy}\} = \{\partial^2 w/\partial x^2, \partial^2 w/\partial y^2, 2\partial^2 w/\partial x\partial y\}$ through the **ABD** relation of Eq. (1), in which, u, v and w are the middle-surface displacements in the x, y and z directions, respectively. Equations (23) can be expressed in terms of these mid-plane displacements as:

$$\begin{aligned}
&A_{11}\partial^2 u/\partial x^2 + A_{66}\partial^2 u/\partial y^2 + (A_{12} + A_{66})\partial^2 v/\partial x\partial y - 3B_{16}\partial^3 w/\partial x^2\partial y - B_{26}\partial^3 w/\partial y^3 = 0\\
&(A_{12} + A_{66})\partial^2 u/\partial x\partial y + A_{66}\partial^2 v/\partial x^2 + A_{22}\partial^2 v/\partial y^2 - B_{16}\partial^3 w/\partial x^3 - 3B_{26}\partial^3 w/\partial x\partial y^2 = 0\\
&D_{11}\partial^4 w/\partial x^4 + 2(D_{12} + 2D_{66})\partial^4 w/\partial x^2\partial y^2 + D_{22}\partial^4 w/\partial y^4 - 3B_{16}\partial^3 u/\partial x^2\partial y - B_{26}\partial^3 u/\partial y^3 -\\
&B_{16}\partial^3 v/\partial x^3 - 3B_{26}\partial^3 v/\partial x\partial y^2 + \rho\partial^2 w/\partial t^2 = 0
\end{aligned} \qquad (24)$$

The free vibration of an elastic plate is harmonic in time, so for an E-T-S-B laminated rectangular plate ($a \times b$) under so called *S3* simply supported boundary conditions [19], which constrain in-plane shearing and remove the possibility of induced shearing-bending coupling, mid-plane displacements are of the form:

$$\begin{aligned}
u &= U\sin(m\pi x/a)\cos(n\pi x/b)e^{i\omega t}\\
v &= V\cos(m\pi x/a)\sin(n\pi x/b)e^{i\omega t}\\
w &= W\sin(m\pi x/a)\sin(n\pi x/b)e^{i\omega t}
\end{aligned} \qquad (25)$$

which satisfy the boundary conditions and equilibrium equations if the circular natural frequency [19]:

$$\omega^2 = (\pi^4/\rho)\{T_{33} + (2T_{12}T_{23}T_{13} - T_{22}T_{13}^2 - T_{11}T_{23}^2)/(T_{11}T_{22} - T_{12}^2)\} \qquad (26)$$

where

$$T_{11} = A_{11}(m\pi/a)^2 + A_{66}(n\pi/b)^2$$

$$T_{12} = (A_{12} + A_{66})(m\pi/a)(n\pi/b)$$

$$T_{13} = -(3B_{16}(m\pi/a)^2 + B_{26}(n\pi/b)^2)(n\pi/b)$$

$$T_{22} = A_{22}(n\pi/b)^2 + A_{66}(m\pi/a)^2$$

$$T_{23} = -(B_{16}(m\pi/a)^2 + 3B_{26}(n\pi/b)^2)(m\pi/a)$$

$$T_{33} = D_{11}(m\pi/a)^4 + 2(D_{12} + 2D_{66})(m\pi/a)^2(n\pi/b)^2 + D_{22}(n\pi/b)^4$$

4. Natural frequency Results.

This section presents bounds on the natural frequencies of *E-T-S-B* coupled: angle-ply laminates (with symmetric and non-symmetric configurations); laminates containing standard ply orientations and; Hygro-Thermally Curvature-Stable laminates.

Due to the substantial number of laminate solutions found, from which upper- and lower-bound natural frequencies envelopes are now derived, the closed form solution of Eq. (26) has been incorporated into a computer code in which the non-dimensional parameters for each stacking sequence, derived in Section 2, are read and a series of natural frequency factor calculations performed over a range of aspect ratios. Such a study would not be possible with a commercial analysis code, but checks using the MSC/NASTRAN® finite element code have been performed to ensure that the results presented here are validated.

4.1 *Benchmark results.*

Table 5 gives the fundamental natural frequency results for the antisymmetric $\mathbf{A_S B_t D_S}$ laminate stacking sequence: $[45°/-45°/45°/-45°]_T$, and with assumed material properties: $E_1/E_2 = 40$, $G_{12}/E_2 = 0.6$, $G_{13} = G_{23} = G_{12}$ and $\nu_{12} = 0.25$. The frequency factor results, Ω', follow from Khdeir [17], which are matched against those calculated with MSC/NASTRAN®. The total thickness of laminate was set to $H = b/1000$ to ensure that the ratios $E_1/G_{13} \times (H/a)^2$ and $E_2/G_{23} \times (H/b)^2$ are approximately equal to zero, hence the effects of shear deformation can be ignored [24]. A converged mesh was achieved using 6400 QUAD4 elements for plate aspect ratio a/b

=1, which was modified for each aspect ratio investigated to maintain a consistent mesh density. Note that non-dimensional frequency factors used elsewhere [16,17], e.g.:

$$\Omega' = \omega a^2/H\sqrt{(\rho'/E_2)} \quad (27)$$

where a is the plate length, H is the laminate thickness and ρ' and E_2 are the material density and Young's modulus, respectively, are appropriate only for the comparison of laminates containing repeating pairs of anti-symmetric angle-plies, and with the explicit constraint that the number of plies can be increased without increasing the laminate thickness. This normalisation procedure is inappropriate for the new results presented here, due to mismatches in bending stiffness contribution in laminates with 2, 3 or 4 ply orientations and/or different forms of stacking sequence symmetry.

The following equation is used to present the non-dimensional results for the composite materials presented throughout this article:

$$\Omega = \omega b^2/\pi^2\sqrt{(\rho/D_{Iso})} \quad (28)$$

where the flexural rigidity, D_{Iso}, for the equivalent isotropic composite material is:

$$D_{Iso} = U_1 H^3/12 \quad (29)$$

with laminate of thickness, H, corresponding to the total number of plies, n, of uniform ply thickness, t. The laminate invariant, U_1, is defined in Eq. (14).

Table 5 provides the MSC/NASTRAN® frequency factor comparisons between, Ω', of Eq. (27), and, Ω, of Eq. (28), for stacking sequence: $[45°/-45°/45°/-45°]_T$, together with the bounds obtained from the closed form solution of Eq. (26), applied to all the stacking sequences within this ply number grouping.

Note that the laminate stacking sequence: $[45°/-45°/45°/-45°]_T$ gives rise to the upper-bound natural frequency envelope across the frequency spectrum investigated, i.e. for the fundamental, 2nd and 3rd natural frequencies. This is a common feature of anti-symmetric angle-ply laminates, which is seen in other comparisons that follow, but is not shared by other forms of laminate, where configurations contained within the upper-bound envelope change with frequency.

The closed form solution of Eq. (26) has also been validated by others [23] through a so called determinantal equation of order five, as part of a study investigating the effects of shear deformation. One of the most striking comparisons given demonstrates the effect of varying angle-ply orientation (θ), which is assumed to be constant ($\theta = 45°$) in the remainder of this study. Jones *et al.* [16], concluded that for anti-symmetric angle-ply plates, the effect of increasing the angle ply orientation (up to 45°) is to increase the fundamental frequency, except for the case of a two layer anti-symmetric angle-ply laminate for which it decreases.

These fundamental frequency design curves have been reproduced in Fig. 2 for the classical plate theory results. The frequency factor result for the equivalent Fully Isotropic Laminate, or FIL, is superimposed for comparison. The anti-symmetric angle-ply laminate $[(+\theta/-\theta)_{n/2}]_T$, or $[+\theta/-\theta/\ldots\ldots/+\theta/-\theta]_T$, was assumed, i.e., the form that is synonymous with the Extension-Twisting (and Shearing-Bending) coupled laminates, where n = 2, 4, 6 and ∞ in the stacking sequence definition represents the total number of plies and also the labelling adopted for the corresponding design curve. The upper-bound curve, representing an infinite number of repetitions of the alternating plies, converges on the fully uncoupled laminate, which in this case represents curve 8a, i.e., the 8-ply laminate $[+\theta/-\theta_2/+\theta]_A$. The upper bound curves for 8 ply laminates with either angle-ply or standard ply orientations are indicated by curves 8b and 8c, respectively. The highest fundamental frequency corresponds to $\theta = 45°$ in all anti-symmetric laminates except for the 2-ply laminate (curve 2), for which the highest fundamental frequency corresponds to $\theta = 0°$. By contrast, the lowest fundamental frequency corresponds to $\theta = 0°$ in all but the 2-ply laminate, for which this occurs at $\theta = \pi/8$ or 22.5°.

Newly derived stacking sequences, which are not constrained by the notion of anti-symmetry and repeating groups, demonstrate a very different picture on Fig. 2. The most significant observations are demonstrated by curves 8d, 8e and 8f. Curve 8d represents the angle-ply laminate $[+\theta_4/-\theta_4]_T$ with 8 layers, which is identical to curve 2, i.e., the 2-ply anti-symmetric laminate. This means that the magnitude of the Extension-Twisting (and Shearing-Bending)

coupling, and hence natural frequency factor, does not necessarily change as the number of plies is increased. Additionally, curve 8e represents the lower-bound solution for the 8-ply laminate $[+\theta_3/0_2/-\theta_3]_T$ with standard ply orientations, whilst curve 8f represents the lower-bound solution for the 8-ply laminate $[+\theta_3/90_2/-\theta_3]_T$. Curves 8e and 8f represent new lower-bound solutions and demonstrate that stacking sequences with alternating angle plies fail to capture the true lower bound solutions for this class of coupled laminate.

The curves also demonstrate that laminates with non-symmetric stacking sequences, and/or those containing standard ply orientations, all of which share the same coupling behaviour, may be found in both the upper and lower-bound envelopes of the fundamental natural frequency design curves.

Upper- and lower-bounds on Hygro-Thermally Curvature-Stable solutions are also shown for 8-ply laminates. These solutions correspond to the points 8g and 8h respectively, since *E-T-S-B* coupling behaviour exists only when the off-axis rotation of the principal material axis, with respect to the structural or system axis, corresponds to $\beta = \pi/8$ or $-\pi/8$; when the principal material axis and structural axis are coincident, i.e., when axis-aligned, the ply orientations correspond to ±45, 90 and/or 0°.

4.2 ***New laminate design comparisons.***

Twelve ply $\mathbf{A_S B_t D_S}$ laminates are now considered in order to demonstrate the difference between upper- and lower-bound natural frequency factors for the 1050 standard laminates and the 35 angle-ply laminates; this is also the lowest ply number grouping in which non-symmetric angle-ply laminates are present, and comparisons are also possible with Hygro-Thermally Curvature-Stable laminates.

Figure 3(a) illustrates the first three natural frequency factor envelopes for Standard laminates, shown by solid lines, with labels $S1^L$ – $S3^L$ and $S1^U$ – $S3^U$, for the lower- and upper-bound envelopes, respectively. These are compared with the corresponding Angle-ply laminate envelopes, shown dotted, with labels $A1^L$ – $A3^L$ and $A1^U$ – $A3^U$. Note that the results

representing Standard laminates contain no angle-ply only results. Envelopes for the equivalent Fully Isotropic Laminate, or FIL, are superimposed for comparison, with labels FIL1 – FIL3. Kinks in the frequency envelopes are due to a change in mode shape.

The lower-bound envelope of the fundamental frequency for Standard laminates is always lower than that for Angle-ply laminates, irrespectively of the aspect ratio. However, the upper bound of the fundamental natural frequency for angle-ply laminates is higher than that for standard laminates when the aspect ratio is close to $a/b = 1.0$. Nevertheless, the difference between the bounds is small, since the Standard laminate stacking sequence is dominated by ±45° plies, with only a central ply block of cross plies (0 or 90°), which do not significant influence on the bending stiffness properties. Upper-bounds for the higher frequencies are generally either coincident, for similar reasons, or higher for the Standard laminate stacking sequences.

The equivalent Fully Isotropic Laminate (FIL) curves are always bounded by the upper- and lower-bound curves for Standard laminates. This is not the case for the Angle-ply laminates, for which the upper-bound curves fall below the FIL curves as the aspect ratio increases and the effect of 90° plies begins to influence the natural frequencies.

Table 6(a) provides a list of the stacking sequences forming the upper- and lower-bound fundamental frequency envelopes in Fig. 3(a), together with the range of applicable aspect ratios. Similar listings are provided in Table 7 for upper-bounds on the higher frequency envelopes with Standard laminates, including details of which of the three natural frequency curves each stacking sequence is associated. By contrast, the angle-ply stacking sequences of Table 6(b) remain unchanged across the frequency spectrum investigated. Whilst the bounds on the fundamental frequency envelopes for Standard laminates are all anti-symmetric stacking sequences, Table 7 reveals that non-symmetric sequences are present in the higher frequency envelopes.

The form of the stacking sequences in the upper bound envelopes, generally involve an interlacing of 45° and -45° plies, which this results in smaller B_{16} and B_{26} terms, hence weaker *Extension-Twisting* coupling. For stacking sequences in the lower bound envelope, the 45° and -45° plies appear as contiguous ply block, anti-symmetrically disposed about the laminate mid-plane, which results in larger B_{16} and B_{26} terms, hence stronger *Extension-Twisting* coupling. The natural frequency is also strongly influenced by the bending stiffness across the shortest side length along which the mode shape develops, which explains why the frequency envelopes of the Angle-ply laminates drop away from those of Standard laminates for both short or long plate aspect ratios.

Tests on higher aspect ratios revealed no changes in the stacking sequences identified in the lists given in Table 6. Additionally, the upper bound fundamental natural frequency factor result for laminate $[-/\bullet/\bullet/\bullet/+/+/-/-/\bullet/\bullet/\bullet/+]_T$, with $\Omega = 1.3162$ at aspect ratio $a/b = 5.0$, reduced by 1.48% at $a/b = 10.0$ and by a further 0.38% at $a/b = 20.0$, which justifies curtailment of the range of aspect ratio presented.

Changes in the frequency factor envelopes are minimal between each ply number grouping. This can be realised only by virtue of the new form of the non-dimensional frequency factor used. Changes arise only as a result of an expansion in the design space with increasing ply number groupings: primarily affecting the bounds on the fundamental natural frequencies, but also resulting in a shift in aspect ratio at which a mode change may occur in the high frequencies. These changes can be readily compared in Figs A1(a) - A4(a) of the electronic annex to this article, which present results for 8, 12, 16 and 20 ply laminates; chosen because these ply number groupings have matching HTCS solutions, which are compared in Figs A1(b) - A4(b). Note that ply number groupings with $2 \leq n \leq 4$ fall significantly below the frequency factor envelopes of all other ply number groupings considered, as was seen in Fig. 2. However, given that such laminates are of limited practical interest, additional information has been

omitted here. Similarly, the intermediate ply number groupings within the range investigated ($n \leq 21$) are also omitted, since they offer little additional insight.

Figure 3(b) illustrates the first three natural frequency factor envelopes for HTCS laminates, which replace the Standard laminate results of Fig. 3(a). They are shown by solid lines, with labels $H1^L$ – $H3^L$ and $H1^U$ – $H3^U$, for the upper- and lower-bound envelopes, respectively. Once again, these are compared with the corresponding Angle-ply laminate envelopes, shown dotted, with labels $A1^L$ – $A3^L$ and $A1^U$ – $A3^U$, and envelopes for the equivalent Fully Isotropic Laminate, or FIL, are superimposed for comparison, with labels FIL1 – FIL3.

The HTCS frequency envelopes form much tighter bounds around the equivalent FIL curves.

In all cases the HTCS lower-bound envelopes lie above those of the Angle-ply and Standard laminates, and always lower than that for the equivalent FIL. However, the relationship between the HTCS upper-bound envelope and those for Standard laminates and the equivalent FIL is more complicated. Indeed, due to the square symmetric stiffness characteristics inherent in HTCS laminates, referred to as bi-axially isotropic by others [19], there is coincidence between the upper bounds $H1^U$, $H2^U$ and $H3^U$ and the FIL1 – FIL3 frequency curves for aspect ratios a/b = 1.0, 2.0 and 3.0; the curves $H2^U$ = FIL2 = 2.00 at a/b = 2.0.

The upper- and lower-bound solutions that form the frequency envelopes of the HTCS laminates of Fig. 3(b) are presented in Table 6(b) for the fundamental frequency, together with their corresponding aspect ratios. Table 8 presents all unique sequences within the first three natural frequency envelopes, including details of which of the three natural frequency curves each stacking sequence is associated. Note that coincident stacking sequences, forming both upper- and lower-bound results, are due to mode changes across the range of aspect ratios investigated.

Figures A1(b) - A4(b) of the electronic annex present additional curves for easy comparison of 8-,12-, 16- and 20-ply HTCS laminates.

5. Conclusions.

New Extension-Twisting and Shearing-Bending coupled laminates, with up to 21 plies, have been derived from combinations of standard ply orientations, i.e., +45, -45, 0 and 90°, and have been shown to exist for all (odd and even) ply number groupings. These results serve to dismiss the long-held misconception that this class of laminate is constrained to even ply number groupings of anti-symmetric Angle-ply laminates.

The design space for Standard laminates, i.e. those containing combination of angle-plies and cross-plies, with standard ply orientations, has been shown to be vast in comparison to the previously assumed anti-symmetric Angle-ply laminate configurations. Non-symmetric Angle-ply configurations have also been identified and fully uncoupled anti-symmetric laminate designs have highlighted the problem of associating sub-sequence symmetry with coupling behaviour. The design space increases yet further with the introduction of Hygo-Thermally Curvature Stable laminates. .

Frequency factor envelopes are presented, which represent upper- and lower-bounds on the first three natural frequencies for rectangular plates, across a broad range of aspect ratios. These have revealed an increase in the bounds for Standard laminate configurations in comparison to Angle-ply (only) laminates; and contain both anti-symmetric and non-symmetric stacking sequences.

Frequency factor envelopes for HTCS laminates have been shown to be constrained within tighter frequency bounds, around the equivalent isotropic laminate, compared to Standard or Angle-ply designs for this class of mechanically coupled laminate. However, HTCS laminates are the only group of designs that can be manufactured flat after high temperature curing.

Acknowledgement.

The authors gratefully acknowledge the support of the National Natural Science Foundation of China (Grant No. 11472003).

References.

1. York, C. B. Characterization of non-symmetric forms of fully orthotropic laminates. J. Aircraft 2009;46:1114-1125.

2. York, C. B. Unified approach to the characterization of coupled composite laminates: Benchmark configurations and special Cases. Journal of Aerospace Engineering, ASCE 2010; 23(4):219-242.

3. York, C. B. Unified approach to the characterization of coupled composite laminates: Hygro-thermally curvature-stable configurations. International Journal of Structural Integrity 2011;2(4):406-436.

4. York, C. B. Tapered hygo-thermally curvature-stable laminates with non-standard ply orientations. Composites Part A: Applied Science and Manufacturing, 2013;44:140-148.

5. York, C. B. On tapered warp-free laminates with single-ply terminations. Composites Part A: Applied Science and Manufacturing, 2015, In Press.

6. Nixon, M. W. Extension-twist coupling of composite circular tubes with application to tilt rotor blade design. Proceedings of the 28th AIAA/ASME/ASCE/AHS/ASC Structures, Structural Dynamics, and Materials Conference, Monterey, USA, 1987.

7. Hill, C. H. and Winckler, S. J. The reduction of environmental effects on tension-twist coupled composite tubes. Journal of Composite Materials 1993;27:1762-1785.

8. Winckler, S. J. Hygrothermally curvature stable laminates with tension-torsion coupling. Journal of the American Helicopter Society 1985;31:56-58.

9. Chen, H. P. Study of hygrothermal isotropic layup and hygrothermal curvature-stable coupling composite laminates. Proceedings of the 44th AIAA/ASME/ASCE/AHS/ASC Structures, Structural Dynamics, and Materials Conference, California, USA, 2003.

10. Cross, R. J., Haynes, R. A. and Armanios, E. A. Families of hygrothermally stable asymmetric laminated composites. Journal of Composite Materials 2008;42:697-716.

11. Haynes R. and Armanios, E. Hygrothermally stable extension-twist coupled laminates with bending-twist coupled laminates. Proceedings of the American Helicopter Society 67th Annual Forum, Virginia, USA, 2011.

12. Reddy, J. N., Khdeir, A. A. and Librescu, L. Lévy type solutions for symmetrically laminated rectangular plates using first-order shear deformation theory. Journal of Applied Mechanics, Transactions of the ASME 1987;54:740-742.

13. Khdeir A. A. and Librescu, L. Analysis of Symmetric Cross-Ply Laminated Elastic Plates Using Higher Order Theory: Part II — Buckling and Free Vibration. Composite Structures 1988;9:406-436.

14. Khdeir, A. A. Free vibration of and buckling of symmetric cross-ply laminated plates by an exact method. Journal of Sound and Vibration1988;126:447-461.

15. Jones, R. M. Buckling and vibration of rectangular unsymmetrically laminated cross-ply plates. AIAA Journal 1973:1626-1632.

16. Jones, R. M., Morgan, H. S. and Whitney, J. M. Buckling and vibration of antisymmetrically laminated angle-ply rectangular plates. Journal of Applied Mechanics 1973;40:1143-1144.

17. Khdeir, A. A. Free vibration of antisymmetric angle-ply laminated plates including various boundary conditions. Journal of Sound and Vibration 1988;122:377-388.

18. Leissa, A. W. Conditions for laminated plates to remain flat under inplane loading. Composite Structures 1986;6:261-270.

19. Jones, R. M. Mechanics of composite materials. London: Taylor and Francis, 1999.

20. Williams, F.W., Ouyang, H.J., Kennedy, D. and York, C. B. Wave propagation along longitudinally periodically supported or stiffened prismatic plate assemblies. Journal of Sound and Vibration 1995;186;197-205.

21. Engineering Sciences Data Unit. Stiffnesses of laminated plates. ESDU Item No. 94003, IHS, 1994.

22. Tsai, S.W., Hahn, H.T. Introduction to composite materials. Technomic Publishing Co. Inc., Lancaster, 1980.

23. Bert C. W. and Chen, T. L. C. Effect of shear deformation on vibration of antisymmetric angle-ply laminated rectangular plates. International Journal of Solids and Structures 1978;14:465-473.

24. Groh, R. M. J. and Weaver, P. M. Static inconsistencies in certain axiomatic higher-order shear deformation theories for beams, plates and shells. Composite Structures 2015; 120: 231-245.

Figures:

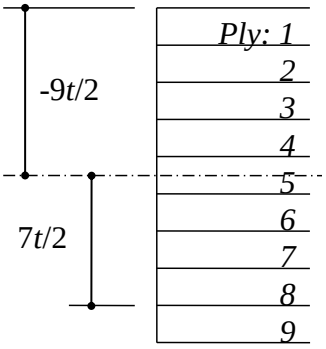

Figure 1 – Laminate cross-section illustrating ply (*k*) numbering scheme and interface distances (*z*) from laminate mid-plane in terms of constant ply thickness, *t*.

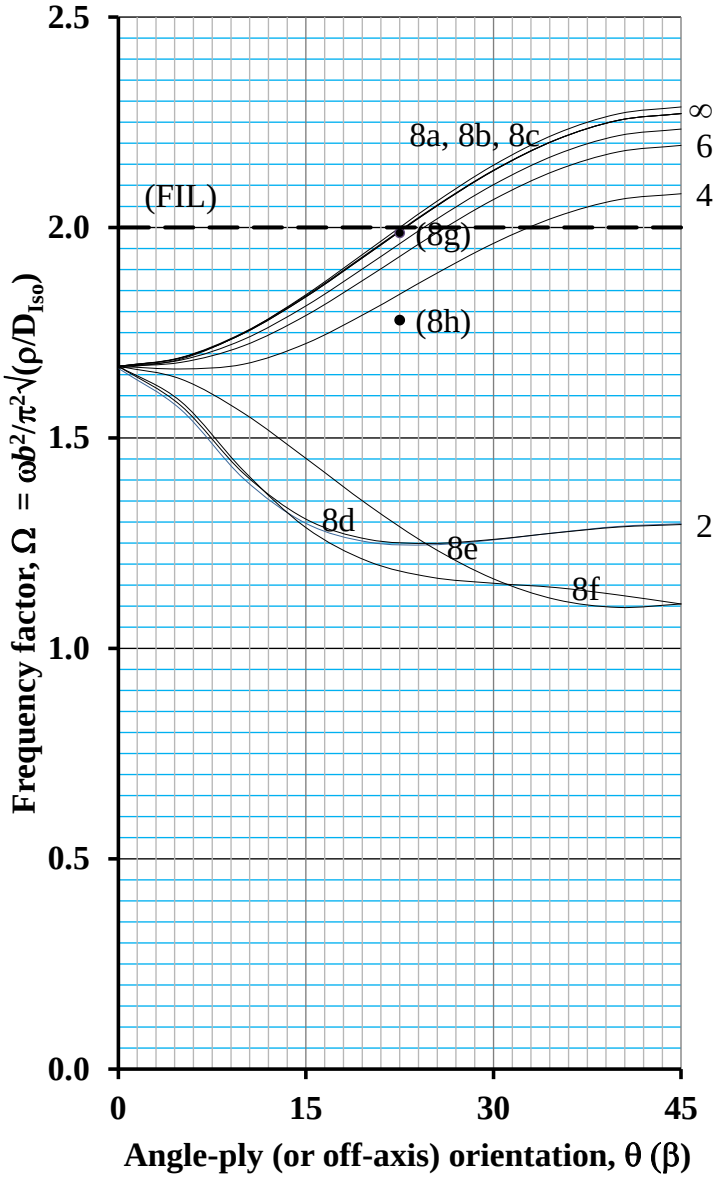

Figure 2 – Frequency factor bounds for a square plate as a function of varying angle-ply orientation, θ, formed by: anti-symmetric Angle-ply laminates with increasing ply number groupings (n = 2,4,6,…, ∞); Standard laminates containing cross-ply and/or angle-combinations (8a – 8f) and; Hygro-Thermally Curvature Stable laminates (8g, 8h) as a result of off-axis orientation, β = 22.5.

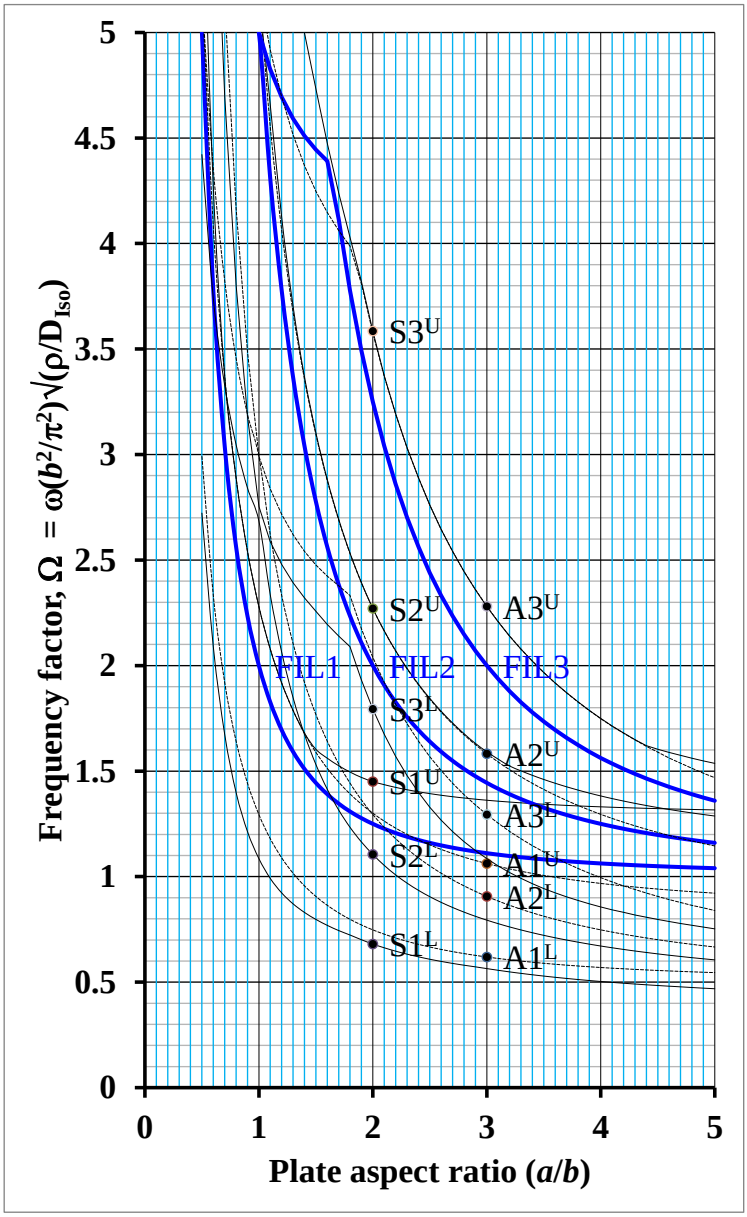

(a)

Figure 3 – Natural frequency factor bounds for 12-ply $\mathbf{A}_S\mathbf{B}_t\mathbf{D}_S$ laminates with angle-ply, A, laminates (broken lines) and: (a) standard, S, laminates (solid lines) or;

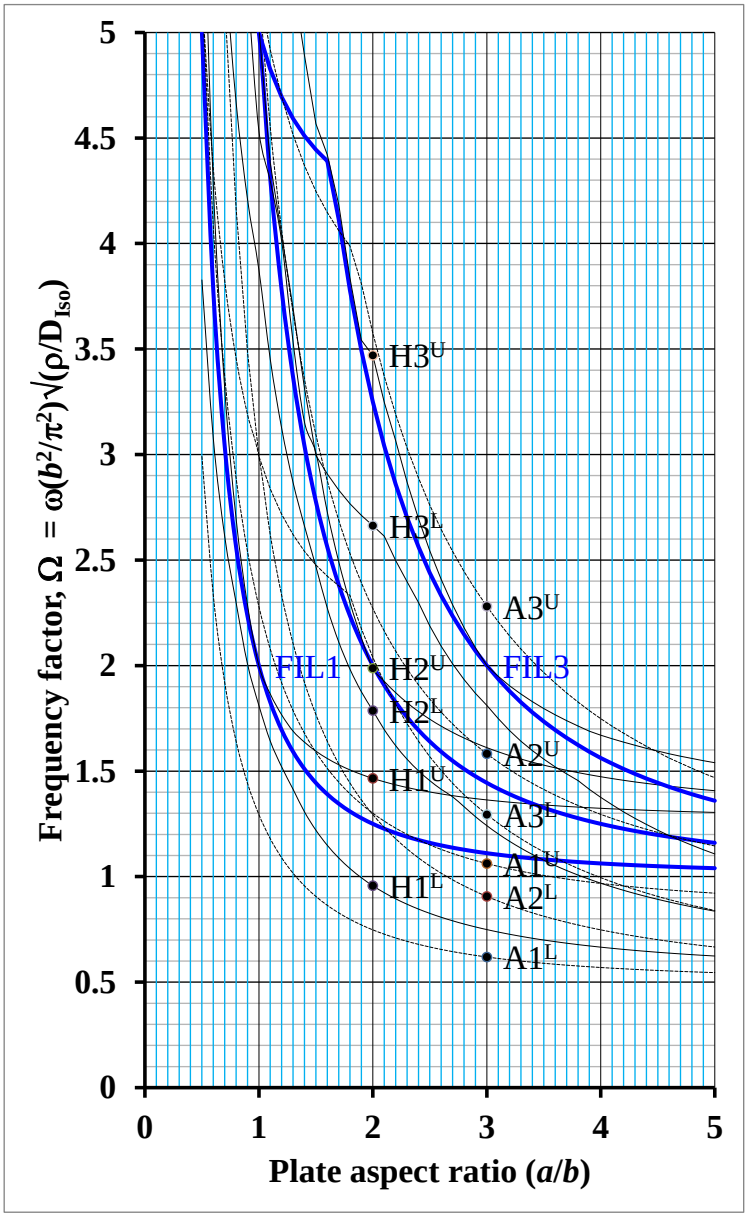

(b)

(b) Hygro-Thermally Curvature Stable, H, laminates (solid lines). The frequency curves for the equivalent fully isotropic laminate, or FIL, are superimposed for comparison. Numbers following the laminate descriptions A, H and S, represent the 1st, 2nd and 3rd natural frequency factors, with superscripts L and U to represent Lower- and Upper-bounds, respectively.

Tables

Table 1 – Number of solutions for $\mathbf{A_S B_t D_S}$ laminates with up to (n =) 21 layers. Standard laminate configurations represent those with combinations of angle-ply and cross-ply (0° and/or 90°) layers. The numbers in parentheses correspond to non-symmetric angle-ply laminate solutions.

n	2	3	4	5	6	7	8	9	10	11	12	13	14	15	16	17	18	19	20	21
Standard	0	2	2	8	12	30	56	128	240	536	1,050	2,412	4,690	11,292	21,800	58,502	111,396	329,412	631,644	2,095,268
Angle-ply	1	-	2	-	4	-	7	-	16	-	35(4)	-	84(20)	-	194(70)	-	512(256)	-	1,352(850)	-

Table 2 – Abridged stacking sequence listing for (n =) 12 layer standard $\mathbf{A}_S\mathbf{B}_i\mathbf{D}_S$ laminates.

Ref	Stacking sequence												Non-dimensional parameters											
													n_+	n_-	$n_○$	$n_●$	χ_+	χ_-	$\chi_○$	$\chi_●$	ζ_+	ζ_-	$\zeta_○$	$\zeta_●$
1	+	+	+	+	+	○	○	−	−	−	−	−	5	5	2	0	70	-70	0	0	860	860	8	0
2	+	+	+	+	+	●	●	−	−	−	−	−	5	5	0	2	70	-70	0	0	860	860	0	8
:																								
99	+	+	○	−	−	○	○	+	+	○	−	−	4	4	4	0	24	-24	0	0	712	712	304	0
100	+	+	○	−	−	−	+	+	+	○	−	−	5	5	2	0	22	-22	0	0	716	716	296	0
:																								
601	+	−	○	○	+	−	○	+	+	+	−	○	4	4	4	0	8	-8	0	0	568	568	592	0
602	+	−	○	○	+	−	−	○	+	+	○	−	4	4	4	0	4	-4	0	0	616	616	496	0
:																								
999	+	●	●	+	●	●	●	●	−	●	●	−	2	2	0	8	32	-32	0	0	440	440	0	848
1000	+	●	●	○	+	+	−	−	○	●	●	−	3	3	2	4	30	-30	0	0	396	396	152	784
:																								
1049	+	●	●	●	●	−	+	●	●	●	●	−	2	2	0	8	20	-20	0	0	368	368	0	992
1050	+	●	●	●	●	●	●	●	●	●	●	−	1	1	0	10	22	-22	0	0	364	364	0	1000

Table 3 – Abridged stacking sequence listing for (n =) 12 layer angle-ply $\mathbf{A}_S\mathbf{B}_t\mathbf{D}_S$ laminate.

Ref	Stacking sequence												Non-dimensional parameters											
													n_+	n_-	$n_\circ$	$n_\bullet$	χ_+	χ_-	$\chi_\circ$	$\chi_\bullet$	ζ_+	ζ_-	$\zeta_\circ$	$\zeta_\bullet$
1	+	+	+	+	+	+	−	−	−	−	−	−	6	6	-	-	72	-72	0	0	864	864	-	-
2	+	+	+	+	+	−	+	−	−	−	−	−	6	6	-	-	68	-68	0	0	864	864	-	-
:																								
9	+	+	−	+	+	+	−	−	−	+	−	−	6	6	-	-	44	-44	0	0	864	864	-	-
10	+	+	−	+	+	−	+	−	−	+	−	−	6	6	-	-	40	-40	0	0	864	864	-	-
:																								
19	+	−	+	+	−	+	−	+	−	−	+	−	6	6	-	-	24	-24	0	0	864	864	-	-
20	+	−	+	+	−	−	+	+	−	−	+	−	6	6	-	-	20	-20	0	0	864	864	-	-
:																								
29	+	−	−	+	−	−	+	+	−	+	+	−	6	6	-	-	-8	8	0	0	864	864	-	-
30	+	−	−	−	+	+	−	+	+	−	−	+	6	6	-	-	-8	8	0	0	864	864	-	-
:																								
34	+	−	−	−	−	+	−	+	+	+	+	−	6	6	-	-	-24	24	0	0	864	864	-	-
35	+	−	−	−	−	−	+	+	+	+	+	−	6	6	-	-	-28	28	0	0	864	864	-	-

Table 4 - Number of HTCS laminates resulting in $\mathbf{A_S B_t D_S}$ after off-axis alignment $\pm\pi/8$ of parent class, $\mathbf{A_I B_S D_F}$ and $\mathbf{A_I B_S D_I}$. Numbers in parentheses represent ply number grouping, *n*.

$\mathbf{A_I B_S D_F}$ (8)	$\mathbf{A_I B_S D_F}$ (12)	$\mathbf{A_I B_S D_F}$ (16)	$\mathbf{A_I B_S D_F}$ (20)	$\mathbf{A_I B_S D_I}$ (16)
6	20	252	3,076	16

Table 5 - Natural frequency factor comparisons, $\Omega' = \omega a^2/H\sqrt{(\rho'/E_2)}$ and $\Omega = \omega b^2/\pi^2\sqrt{(\rho/D_{Iso})}$ for simply supported rectangular plates with different aspect ratio (*a*/*b*), for a $[45°/-45°/45°/-45°]_T$ laminate, representing : (a) fundamental; (b) 2nd and; (c) 3rd natural frequencies. Results from Eq. (26) represent upper- (Ω^U) and lower-bound (Ω^L) solutions for ply number grouping $n = 4$.

(a)

	Ref. [17]	MSC/NASTRAN®		Eq. (26)	
a/*b*	Ω'	Ω'	Ω	Ω^U	Ω^L
1	23.53	23.46	2.0801	2.0801	1.2941
2	53.74	53.65	1.1878	1.1878	0.7477
3	98.87	98.78	0.9713	0.9713	0.6192

(b)

	Ref. [17]	MSC/NASTRAN®		Eq. (26)	
a/*b*	Ω'	Ω'	Ω	Ω^U	Ω^L
1	53.74	53.6	4.7514	4.7514	2.991
2	94.11	93.89	2.0801	2.0801	1.2941
3	147.65	147.38	1.4504	1.4504	0.9062

(c)

	Ref. [17]	MSC/NASTRAN®		Eq. (26)	
a/*b*	Ω'	Ω'	Ω	Ω^U	Ω^L
1	53.74	53.6	4.7514	4.7514	2.991
2	147.65	147.31	3.2634	3.2634	2.039
3	211.75	211.31	2.0801	2.0801	1.2941

Table 6 – Stacking sequences corresponding to upper and lower bound curves of the fundamental frequency factors of Fig. 3 for: (a) standard; (b) angle-ply and; (c) HTCS $\mathbf{A}_S\mathbf{B}_t\mathbf{D}_S$ laminates.

(a)

a/*b*	Upper-bound	*a*/*b*	Lower-bound
0.5	$[+/○/○/○/–/–/+/+/○/○/○/–]_T$	0.5	$[+/+/+/+/+/○/○/–/–/–/–/–]_T$
0.6	$[+/○/○/–/–/–/+/+/+/○/○/–]_T$	0.6	$[+/+/+/+/○/○/○/○/–/–/–/–]_T$
0.7-0.9	$[+/–/+/–/–/○/○/+/+/–/+/–]_T$	0.7-0.9	$[+/+/+/+/●/●/●/●/–/–/–/–]_T$
1.0-1.4	$[+/–/+/–/–/●/●/+/+/–/+/–]_T$	1.0-1.5	$[+/+/+/+/○/○/○/○/–/–/–/–]_T$
1.5-1.9	$[+/●/●/–/–/–/+/+/+/●/●/–]_T$	1.6-1.8	$[+/+/+/+/●/●/●/●/–/–/–/–]_T$
2.0-5.0	$[+/●/●/●/–/–/+/+/●/●/●/–]_T$	1.9-2.9	$[+/+/+/+/+/●/●/–/–/–/–/–]_T$
		3.0-4.6	$[+/+/+/+/○/○/○/○/–/–/–/–]_T$
		4.7-5.0	$[+/○/+/+/○/○/○/○/–/–/○/–]_T$

(b)

a/*b*	Upper-bound	*a*/*b*	Lower-bound
0.5-5.0	$[+/–/–/+/–/+/–/+/–/+/+/–]_T$	0.5-5.0	$[+/+/+/+/+/+/–/–/–/–/–/–]_T$

(c)

a/*b*	Upper-bound	*a*/*b*	Lower-bound
0.5-0.7	$[+/○/+/–/–/–/●/●/●/○/+/○]_T$	0.5-0.7	$[+/●/+/–/–/–/○/○/○/●/+/●]_T$
0.8-0.9	$[+/○/●/○/–/–/●/●/+/–/+/○]_T$	0.8-0.9	$[+/–/+/–/–/●/+/○/○/●/○/●]_T$
1.0	$[+/○/●/–/–/○/+/●/●/–/+/○]_T$	1.0-1.2	$[+/–/+/–/–/○/+/●/●/○/●/○]_T$
1.1-1.3	$[+/●/○/●/–/–/○/○/+/–/+/●]_T$	1.3-5.0	$[+/○/+/–/–/–/●/●/●/○/+/○]_T$
1.4-5.0	$[+/●/+/–/–/–/○/○/○/●/+/●]_T$		

Table 7 – Stacking sequences corresponding to the 23 unique 12-ply Standard laminates forming one or more of the first three natural frequency upper-bound envelopes of Fig. 3(a); identified by the corresponding numbers in parentheses.

Upper-bound	(Frequency)	Upper-bound	(Frequency)
$[+/O/O/O/-/-/-]_A$	(1)	$[+/O/-/-/●/●]_A$	(3)
$[+/O/O/-/-/-/-]_A$	(1)	$[+/-/O/O/O/O/+/-/O/+/-/O]_T$	(3)
$[+/-/+/-/-/O]_A$	(1,2,3)	$[+/O/O/-/O/-]_A$	(3)
$[+/-/+/-/-/●]_A$	(1,2,3)	$[+/●/-/●/-/O]_A$	(3)
$[+/●/●/-/-/-]_A$	(1,2,3)	$[+/●/-/-/+/O]_A$	(3)
$[+/●/●/●/-/-]_A$	(1,2,3)	$[+/-/●/-/●/+]_A$	(3)
$[+/-/●/●/●/-/]_A$	(2)	$[+/-/●/O/-/●]_A$	(3)
$[+/-/-/●/●/+]_A$	(2)	$[+/-/-/●/O/+]_A$	(3)
$[+/-/-/O/+/-/+/+/O/-/-/+]_T$	(2,3)	$[+/-/-/+/●/-]_A$	(3)
$[+/-/O/-/O/+/]_A$	(2)	$[+/-/-/+/O/-]_A$	(3)
$[+/O/-/-/O/O]_A$	(2)	$[+/●/-/●/-/●]_A$	(3)
$[+/-/-/●/+/-/+/+/●/-/-/+]_T$	(3)		

Table 8 – Stacking sequences corresponding to the unique 12-ply HTCS laminates forming one or more of the first three upper-bound and/or lower-bound natural frequency envelopes of Fig. 3(b); identified by the corresponding numbers in parentheses.

Upper-bound	(Frequency)	Lower-bound	(Frequency)
$[+/O/-/+/+/+/●/●/●/O/-/O]_T$	(1,2,3)	$[+/●/-/+/+/+/O/O/O/●/-/●]_T$	(1,2,3)
$[+/O/●/O/+/+/●/●/-/+/-/O]_T$	(1,2,3)	$[+/+/-/+/+/●/-/O/O/●/O/●]_T$	(1,2,3)
$[+/O/●/+/+/O/-/●/●/+/-/O]_T$	(1,2,3)	$[+/+/-/+/+/O/-/●/●/O/●/O]_T$	(1,2,3)
$[+/●/O/●/+/+/O/O/-/+/-/●]_T$	(1,2,3)	$[+/O/-/+/+/+/●/●/●/O/-/O]_T$	(1,2,3)
$[+/●/-/+/+/+/O/O/O/●/-/●]_T$	(1,2,3)	$[+/●/O/+/●/+/O/-/O/+/-/●]_T$	(3)
$[+/●/O/+/●/+/O/-/O/+/-/●]_T$	(2,3)	$[+/+/-/+/●/+/O/-/O/●/O/●]_T$	(3)
$[+/+/-/+/●/+/O/-/O/●/O/●]_T$	(2)	$[+/+/●/O/+/O/-/●/-/+/●/O]_T$	(3)
$[+/+/●/O/+/O/-/●/-/+/●/O]_T$	(2,3)	$[+/+/-/O/+/+/●/●/-/O/●/O]_T$	(3)
$[+/+/●/O/O/+/●/-/-/+/●/O]_T$	(2,3)	$[+/O/●/O/+/+/●/●/-/+/-/O]_T$	(3)
$[+/O/●/+/O/+/●/-/●/+/-/O]_T$	(2,3)		
$[+/●/O/+/+/●/-/O/O/+/-/●]_T$	(3)		
$[+/+/O/●/+/●/-/O/-/+/O/●]_T$	(3)		
$[+/+/-/+/O/+/●/-/●/O/●/O]_T$	(3)		
$[+/+/O/●/●/+/O/-/-/+/O/●]_T$	(3)		

Electronic Annex

This section presents a proof for the non-dimensional constraints used in the development of the *Extension- Twisting* (and *Shearing-Bending*) coupled ($A_S B_t D_S$) laminates presented in the main body of the article, together with additional design curves for the frequency bounds on 8-, 16- and 20-ply laminates, representing Standard, Angle-ply and Hygro-Thermally Curvature Stable (HTCS) or warp-free laminate designs. The 12-ply laminate results from the main body of the article are repeated for completeness.

Proof for non-dimensional design constraints

Elements of the stiffness matrices are related to lamination parameters and laminate invariants, originally conceived by Tsai and Hahn [22], by:

$$
\begin{aligned}
A_{11} &= \{U_1 + \xi_1 U_2 + \xi_2 U_3\} \times H \\
A_{12} = A_{21} &= \{-\xi_2 U_3 + U_4\} \times H \\
A_{16} = A_{61} &= \{\xi_3 U_2/2 + \xi_4 U_3\} \times H \\
A_{22} &= \{U_1 - \xi_1 U_2 + \xi_2 U_3\} \times H \\
A_{26} = A_{62} &= \{\xi_3 U_2/2 - \xi_4 U_3\} \times H \\
A_{66} &= \{-\xi_2 U_3 + U_5\} \times H
\end{aligned}
\tag{A1}
$$

$$
\begin{aligned}
B_{11} &= \{\xi_5 U_2 + \xi_6 U_3\} \times H^2/4 \\
B_{12} = B_{21} &= \{-\xi_6 U_3\} \times H^2/4 \\
B_{16} = B_{61} &= \{\xi_7 U_2/2 + \xi_8 U_3\} \times H^2/4 \\
B_{22} &= \{-\xi_5 U_2 + \xi_6 U_3\} \times H^2/4 \\
B_{26} = B_{62} &= \{\xi_7 U_2/2 - \xi_8 U_3\} \times H^2/4 \\
B_{66} &= \{-\xi_6 U_3\} \times H^2/4
\end{aligned}
\tag{A2}
$$

and

$$
\begin{aligned}
D_{11} &= \{U_1 + \xi_9 U_2 + \xi_{10} U_3\} \times H^3/12 \\
D_{12} = D_{21} &= \{U_4 - \xi_{10} U_3\} \times H^3/12 \\
D_{16} = D_{61} &= \{\xi_{11} U_2/2 + \xi_{12} U_3\} \times H^3/12 \\
D_{22} &= \{U_1 - \xi_9 U_2 + \xi_{10} U_3\} \times H^3/12 \\
D_{26} = D_{62} &= \{\xi_{11} U_2/2 - \xi_{12} U_3\} \times H^3/12 \\
D_{66} &= \{-\xi_{10} U_3 + U_5\} \times H^3/12
\end{aligned}
\tag{A3}
$$

where the U_i are calculated from the reduced stiffness terms, Q_{ij}, of Eq. (14) in the main body of the article.

These ply orientation dependent lamination parameters of are related to the non-dimensional parameters of Eqs (9) – (11) by the following expressions:

$$\xi_1 = \xi_1^{A} = \{n_+\cos(2\theta_+) + n_-\cos(2\theta_-) + n_o\cos(2\theta_o) + n_\bullet\cos(2\theta_\bullet)\}/n$$

$$\xi_2 = \xi_2^{A} = \{n_+\cos(4\theta_+) + n_-\cos(4\theta_-) + n_o\cos(4\theta_o) + n_\bullet\cos(4\theta_\bullet)\}/n$$

$$\xi_3 = \xi_3^{A} = \{n_+\sin(2\theta_+) + n_-\sin(2\theta_-) + n_o\sin(2\theta_o) + n_\bullet\sin(2\theta_\bullet)\}/n \qquad \text{(A4)}$$

$$\xi_4 = \xi_4^{A} = \{n_+\sin(4\theta_+) + n_-\sin(4\theta_-) + n_o\sin(4\theta_o) + n_\bullet\sin(4\theta_\bullet)\}/n$$

$$\xi_5 = \xi_1^{B} = \{\chi_+\cos(2\theta_+) + \chi_-\cos(2\theta_-) + \chi_o\cos(2\theta_o) + \chi_\bullet\cos(2\theta_\bullet)\}/n^2$$

$$\xi_6 = \xi_2^{B} = \{\chi_+\cos(4\theta_+) + \chi_-\cos(4\theta_-) + \chi_o\cos(4\theta_o) + \chi_\bullet\cos(4\theta_\bullet)\}/n^2$$

$$\xi_7 = \xi_3^{B} = \{\chi_+\sin(2\theta_+) + \chi_-\sin(2\theta_-) + \chi_o\sin(2\theta_o) + \chi_\bullet\sin(2\theta_\bullet)\}/n^2 \qquad \text{(A5)}$$

$$\xi_8 = \xi_4^{B} = \{\chi_+\sin(4\theta_+) + \chi_-\sin(4\theta_-) + \chi_o\sin(4\theta_o) + \chi_\bullet\sin(4\theta_\bullet)\}/n^2$$

$$\xi_9 = \xi_1^{D} = \{\zeta_+\cos(2\theta_+) + \zeta_-\cos(2\theta_-) + \zeta_o\cos(2\theta_o) + \zeta_\bullet\cos(2\theta_\bullet)\}/n^3$$

$$\xi_{10} = \xi_2^{D} = \{\zeta_+\cos(4\theta_+) + \zeta_-\cos(4\theta_-) + \zeta_o\cos(4\theta_o) + \zeta_\bullet\cos(4\theta_\bullet)\}/n^3$$

$$\xi_{11} = \xi_3^{D} = \{\zeta_+\sin(2\theta_+) + \zeta_-\sin(2\theta_-) + \zeta_o\sin(2\theta_o) + \zeta_\bullet\sin(2\theta_\bullet)\}/n^3 \qquad \text{(A6)}$$

$$\xi_{12} = \xi_4^{D} = \{\zeta_+\sin(4\theta_+) + \zeta_-\sin(4\theta_-) + \zeta_o\sin(4\theta_o) + \zeta_\bullet\sin(4\theta_\bullet)\}/n^3$$

For $A_S B_t D_S$ laminates, the elements of the stiffness matrices should satisfy the following constraints:

$$A_{16} = A_{26} = 0$$

$$B_{11} = B_{12} = B_{22} = B_{66} = 0 \qquad \text{(A7)}$$

$$B_{16},\ B_{26} \neq 0$$

$$D_{16} = D_{26} = 0$$

Inserting the constraints of Eq. (A7) into Eqs (A1) - (A3) gives:

$$A_{16} = A_{26} = 0 \qquad \rightarrow \xi_3 = \xi_4 = 0$$

$$B_{11} = B_{12} = B_{22} = B_{66} = 0 \qquad \rightarrow \xi_5 = \xi_6 = 0$$

$$B_{16} \neq 0 \qquad \rightarrow \{\xi_7 U_2/2 + \xi_8 U_3\} \neq 0 \qquad \text{(A8)}$$

$$B_{26} \neq 0 \qquad \rightarrow \{\xi_7 U_2/2 - \xi_8 U_3\} \neq 0$$

$$D_{16} = D_{26} = 0 \qquad \rightarrow \xi_{11} = \xi_{12} = 0$$

The lamination parameters for $A_S B_t D_S$ laminates should therefore satisfy the following constraints:

$$\xi_3 = \xi_4 = 0$$

$$\xi_5 = \xi_6 = 0 \qquad\qquad \xi_7 \neq 0,\ \xi_8 \neq 0 \qquad\qquad \text{(A9)}$$

$$\xi_{11} = \xi_{12} = 0$$

Applying the lamination parameter constraints of Eq. (A9) to the lamination parameters of Eqs (A4) – (A6), for laminates containing 0° and 90° cross plies and angle plies with arbitrary orientations ±θ°, gives:

$$\xi_3 = \{n_+\sin(2\theta_+) + n_-\sin(2\theta_-) + n_0\sin(2\times 0) + n_{90^\circ}\sin(2\times 90)\}/n$$

$$\xi_3 = \{n_+\sin(2\theta_+) + n_-\sin(2\theta_-)\}/n = 0 \qquad \rightarrow n_+ = n_-$$

$$\xi_4 = \{n_+\sin(4\theta_+) + n_-\sin(4\theta_-) + n_0\sin(4\times 0) + n_{90^\circ}\sin(4\times 90)\}/n \qquad \text{(A10)}$$

$$\xi_4 = \{n_+\sin(4\theta_+) + n_-\sin(4\theta_-)\}/n = 0 \qquad \rightarrow n_+ = n_-$$

$$\xi_5 = \{\chi_+\cos(2\theta_+) + \chi_-\cos(2\theta_-) + \chi_0\cos(2\times 0) + \chi_{90}\cos(2\times 90)\}/n^2$$

$$\{(\chi_+ + \chi_-)\cos(2\theta_+) + \chi_0 - \chi_{90}\}/n^2 = 0 \qquad \rightarrow (\chi_+ + \chi_-)\cos(2\theta_+) + \chi_0 - \chi_{90} = 0$$

$$\xi_6 = \{\chi_+\cos(4\theta_+) + \chi_-\cos(4\theta_-) + \chi_0\cos(4\times 0) + \chi_{90}\cos(4\times 90)\}/n^2$$

$$\{(\chi_+ + \chi_-)\cos(4\theta_+) + \chi_0 + \chi_{90}\}/n^2 = 0 \qquad \rightarrow (\chi_+ + \chi_-)\cos(4\theta_+) + \chi_0 + \chi_{90} = 0 \qquad \text{(A11)}$$

$$\xi_7 = \{\chi_+\sin(2\theta_+) + \chi_-\sin(2\theta_-) + \chi_0\sin(2\times 0) + \chi_{90}\sin(2\times 90)\}/n^2$$

$$(\chi_+ + \chi_-)\sin(2\theta_-)/n^2 \neq 0 \qquad \rightarrow \chi_+ \neq \chi_-$$

$$\xi_8 = \{\chi_+\sin(4\theta_+) + \chi_-\sin(4\theta_-) + \chi_0\sin(4\times 0) + \chi_{90}\sin(4\times 90)\}/n^2$$

$$(\chi_+ + \chi_-)\sin(4\theta_-)/n^2 \neq 0 \qquad \rightarrow \chi_+ \neq \chi_-$$

$$\xi_{11} = \{\zeta_+\sin(2\theta_+) + \zeta_-\sin(2\theta_-) + \zeta_0\sin(2\times 0) + \zeta_{90^\circ}\sin(2\times 90)\}/n$$

$$\xi_{11} = (\zeta_+ - \zeta_-)\sin(2\theta_+)/n^3 = 0 \qquad \rightarrow \zeta_+ = \zeta_-$$

$$\xi_{12} = \{\zeta_+\sin(4\theta_+) + \zeta_-\sin(4\theta_-) + \zeta_0\sin(4\times 0) + \zeta_{90^\circ}\sin(4\times 90)\}/n^3 \qquad \text{(A12)}$$

$$\xi_{12} = (\zeta_+ - \zeta_-)\sin(4\theta_+)/n^3 = 0 \qquad \rightarrow \zeta_+ = \zeta_-$$

Therefore, $A_SB_tD_S$ laminates should satisfy the following non-dimensional parameter constraints when angle-plies (+/–) can be assigned any arbitrary orientation, $0 < \theta < 90°$, and the cross-plies (○/●, representing 0°/90°) can be interchanged:

$n_+ = n_-$

$(\chi_+ + \chi_-)\cos(2\theta) + \chi_\circ - \chi_\bullet = 0$

$(\chi_+ + \chi_-)\cos(4\theta) + \chi_\circ + \chi_\bullet = 0$ (A13)

$\chi_+ \neq \chi_-$

$\zeta_+ = \zeta_-$

or

$n_+ = n_-$

$\chi_+ = -\chi_-$

$\chi_\circ = \chi_\bullet = 0$ (A14)

$\zeta_+ = \zeta_-$

Design curves for the frequency bounds.

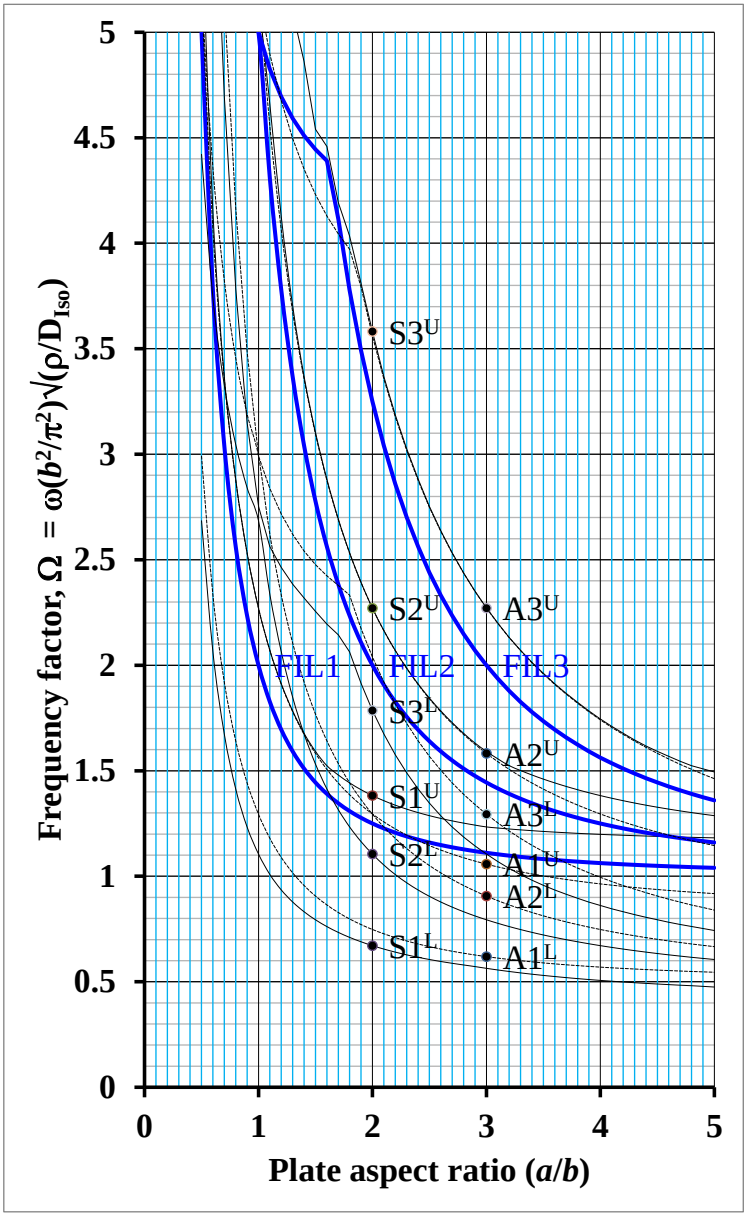

(a)

Figure A1 – Natural frequency factor bounds for 8-ply $\mathbf{A}_S\mathbf{B}_t\mathbf{D}_S$ laminates with angle-ply, A, laminates (broken lines) and: (a) standard, S, laminates (solid lines) or;

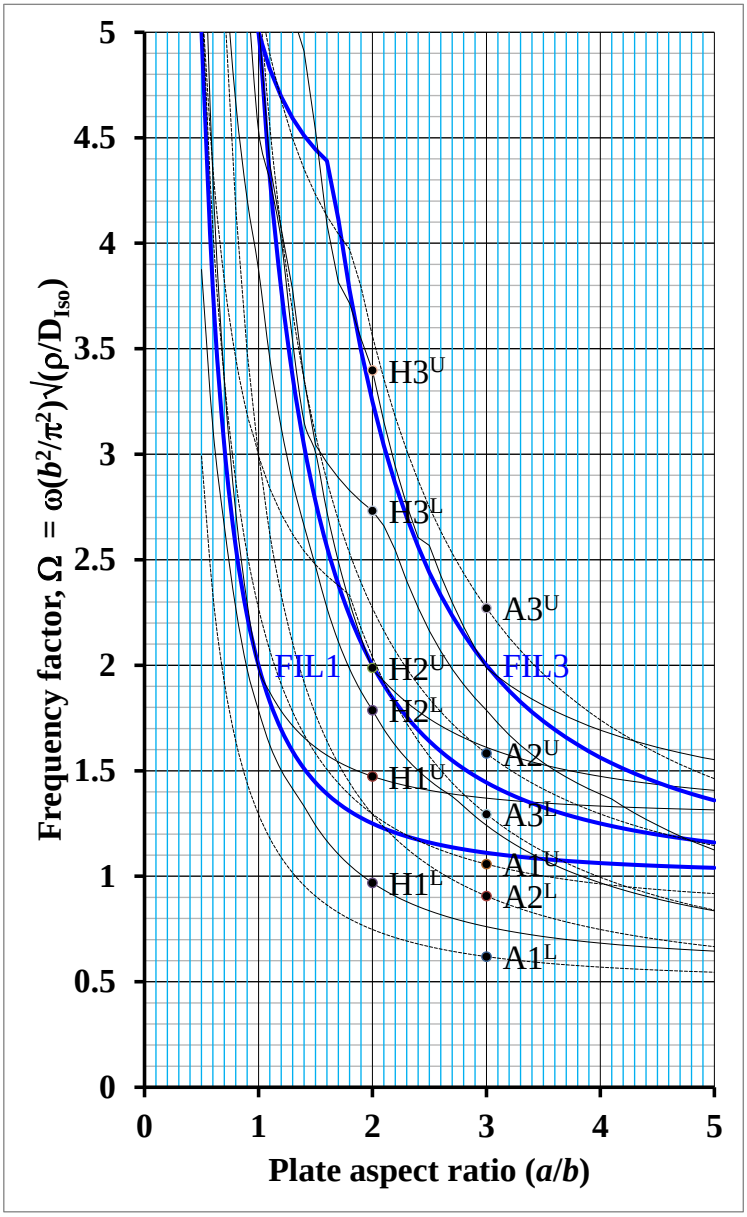

(b)

(b) Hygro-Thermally Curvature Stable, H, laminates (solid lines). The frequency curves for the equivalent fully isotropic laminate, or FIL, are superimposed for comparison. Numbers following the laminate descriptions A, H and S, represent the Fundamental, 2nd and 3rd natural frequency factors, with superscripts L and U to represent Lower- and Upper-bounds, respectively.

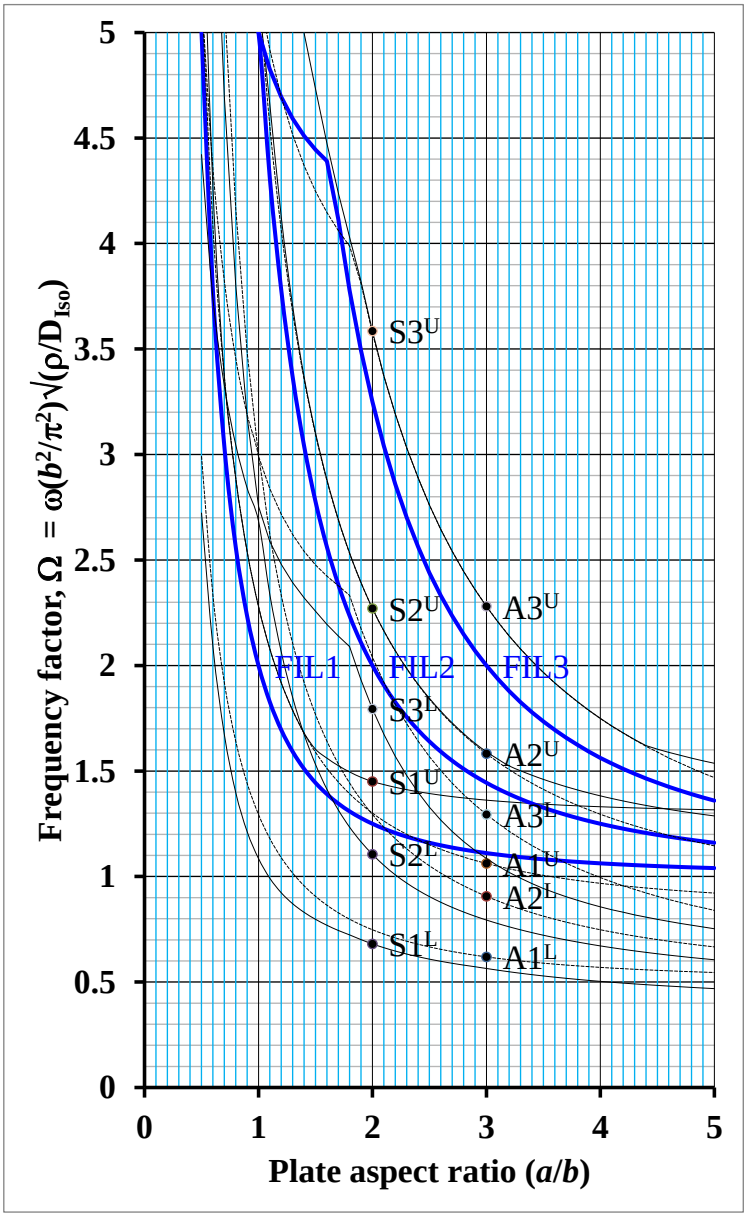

(a)

Figure A2 – Natural frequency factor bounds for 12-ply $\mathbf{A}_S\mathbf{B}_t\mathbf{D}_S$ laminates with angle-ply, A, laminates (broken lines) and: (a) standard, S, laminates (solid lines) or;

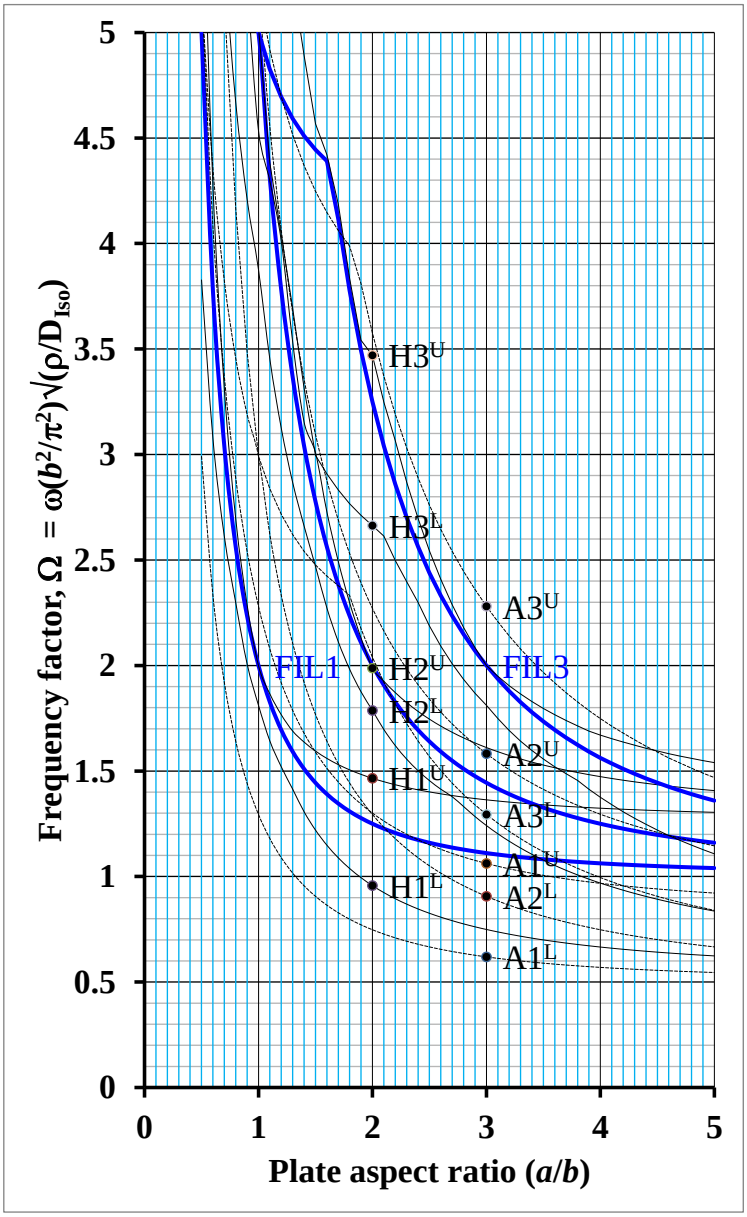

(b)

(b) Hygro-Thermally Curvature Stable, H, laminates (solid lines). The frequency curves for the equivalent fully isotropic laminate, or FIL, are superimposed for comparison. Numbers following the laminate descriptions A, H and S, represent the Fundamental, 2nd and 3rd natural frequency factors, with superscripts L and U to represent Lower- and Upper-bounds, respectively.

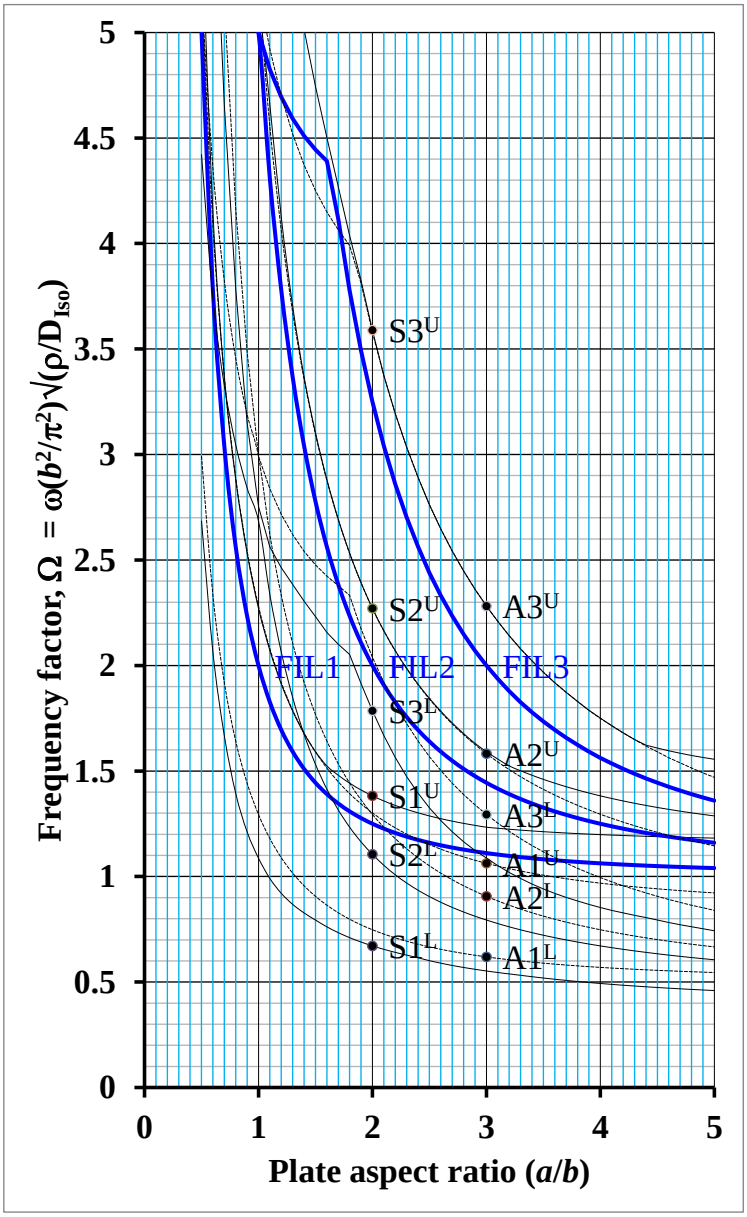

(a)

Figure A3 – Natural frequency factor bounds for 16-ply $\mathbf{A}_S\mathbf{B}_t\mathbf{D}_S$ laminates with angle-ply, A, laminates (broken lines) and: (a) standard, S, laminates (solid lines) or;

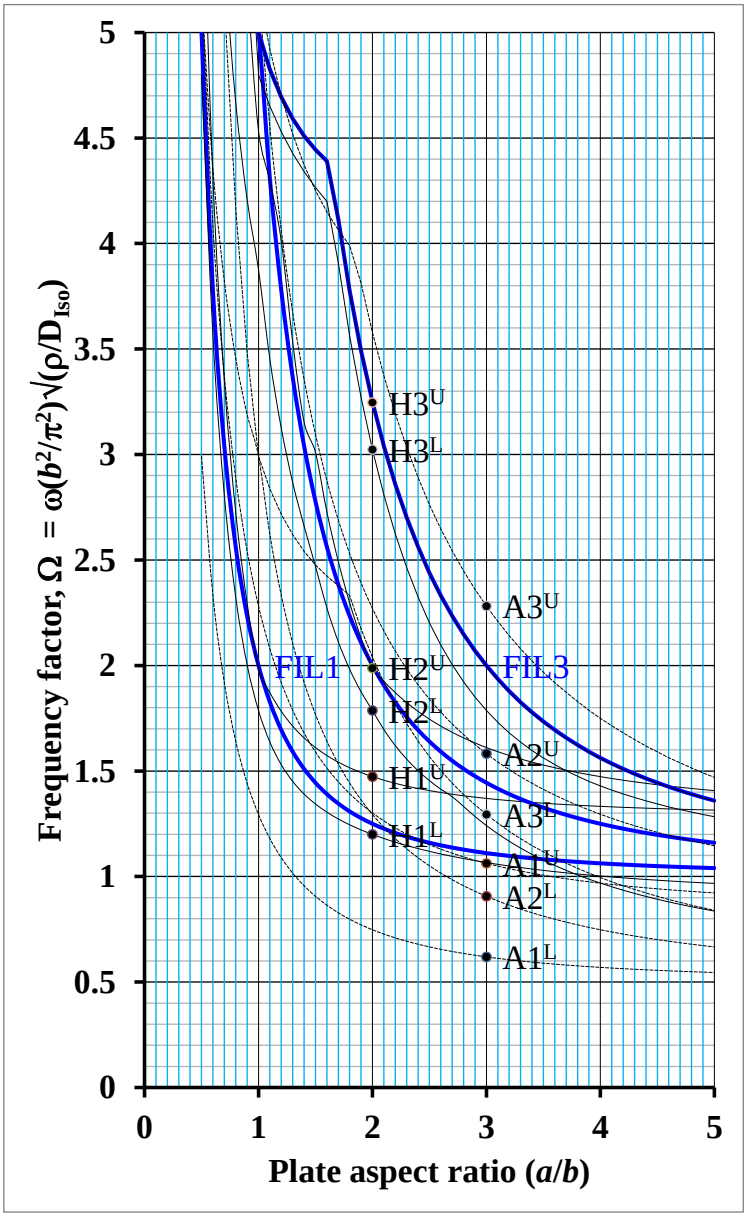

(b)

(b) Hygro-Thermally Curvature Stable, H, laminates (solid lines). The frequency curves for the equivalent fully isotropic laminate, or FIL, are superimposed for comparison. Numbers following the laminate descriptions A, H and S, represent the 1st, 2nd and 3rd natural frequency factors, with superscripts L and U to represent Lower- and Upper-bounds, respectively.

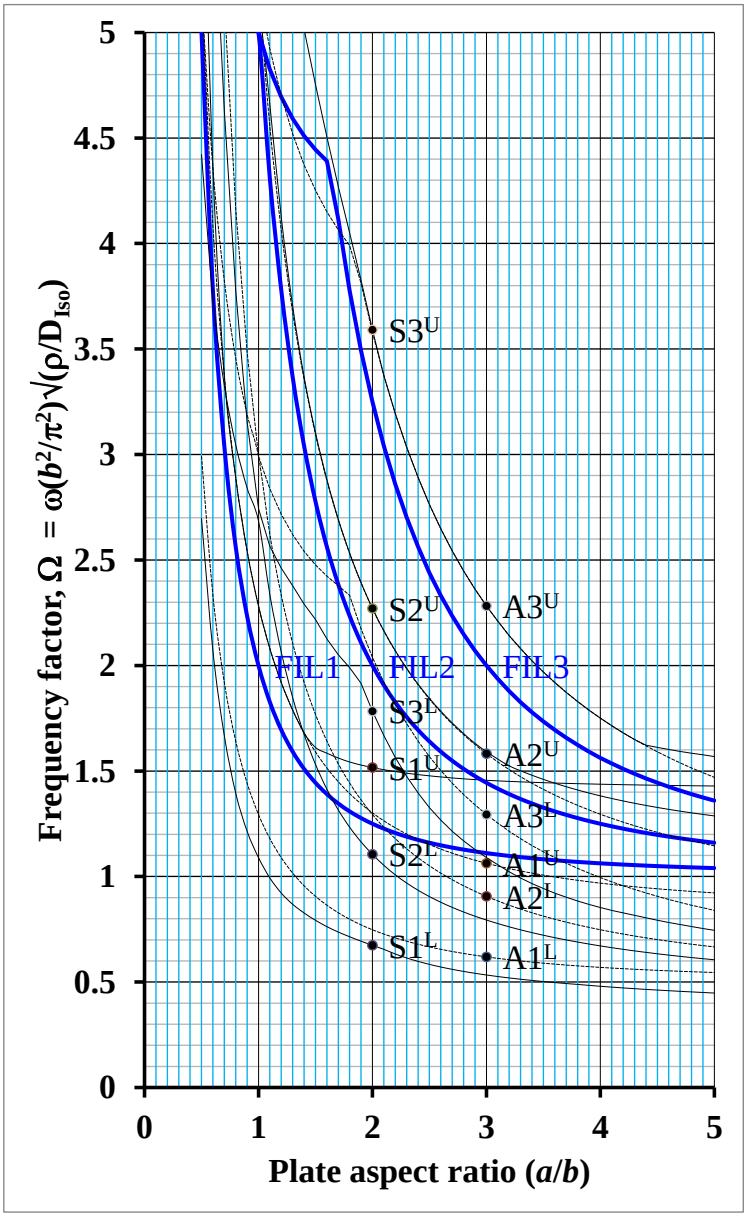

(a)

Figure A4 – Natural frequency factor bounds for 20-ply $\mathbf{A}_S\mathbf{B}_t\mathbf{D}_S$ laminates with angle-ply, A, laminates (broken lines) and: (a) standard, S, laminates (solid lines) or;

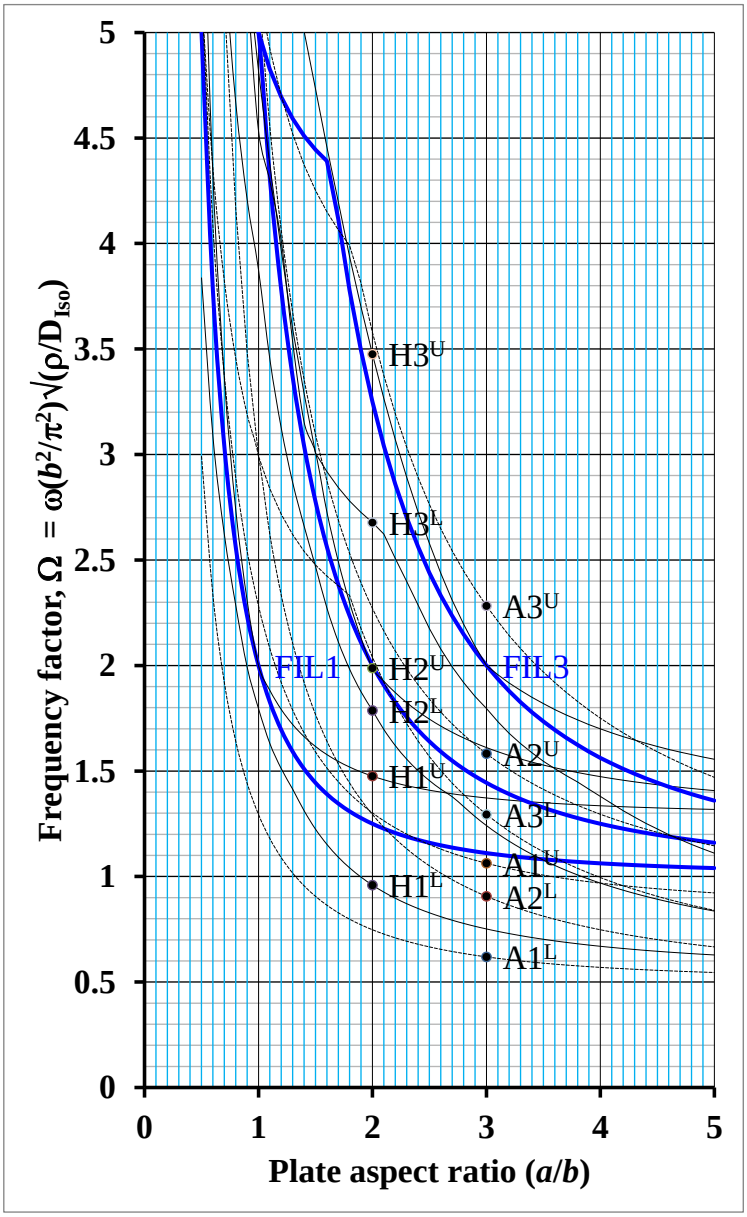

(b)

(b) Hygro-Thermally Curvature Stable, H, laminates (solid lines). The frequency curves for the equivalent fully isotropic laminate, or FIL, are superimposed for comparison. Numbers following the laminate descriptions A, H and S, represent the 1st, 2nd and 3rd natural frequency factors, with superscripts L and U to represent Lower- and Upper-bounds, respectively.